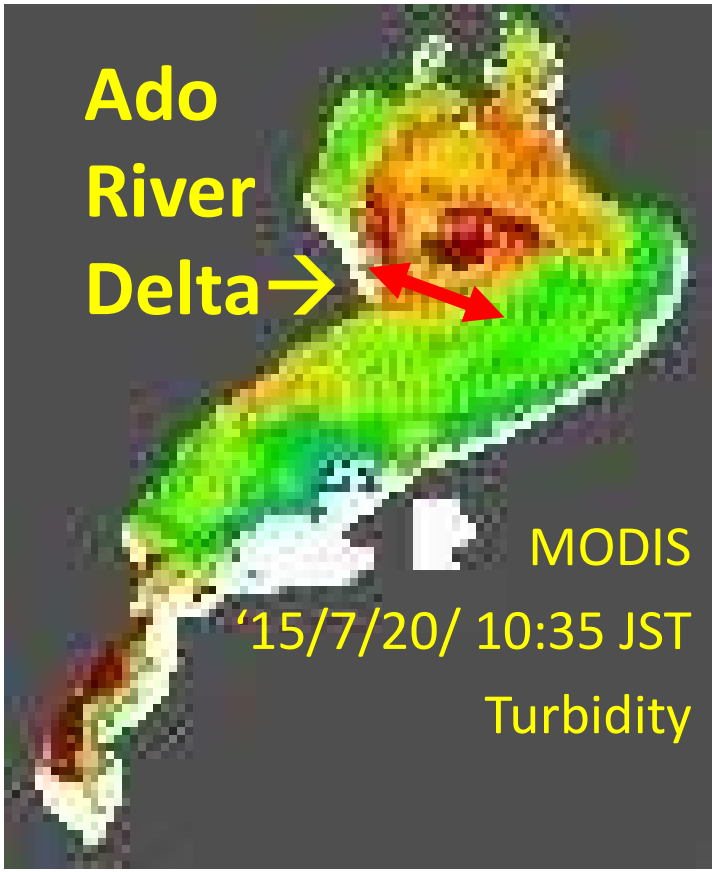
John WELLS ,
Ritsumeikan Univ.

E. UZHANSKY,
Naval Postgrad Schl.

N. TANIGUCHI
Hiroshima Univ.

Acoustic Tomography in a Stratified Lake with Application of the Matched Nonreciprocity Method

We present results from Coastal Acoustic Tomography (CAT) at horizontal ranges up to 14 km believed to be the first field demonstration of CAT in a lake at superkilometer ranges.



Ultimate **target**: track currents *etc.*, thence motion of pollutant, *etc.*, by assimilating CAT data into an operational forecast system.

SynObs Mutsu Aug. 24, 2026

Long-term Aim: Assimilate Information on Acoustic Travel Time into Hydrodynamic simulations

From pairs of transducers ("TR") in acoustic tomography (CAT) network:

→ Average travel times constrain average sound speed (-> avg. temp)

→ **Differential travel times ("DTT") relate to average parallel currents**

Coastal acoustic tomography ("CAT") is complicated by **multiple bottom reflections**, fade-in/out from interference of multipaths, ...

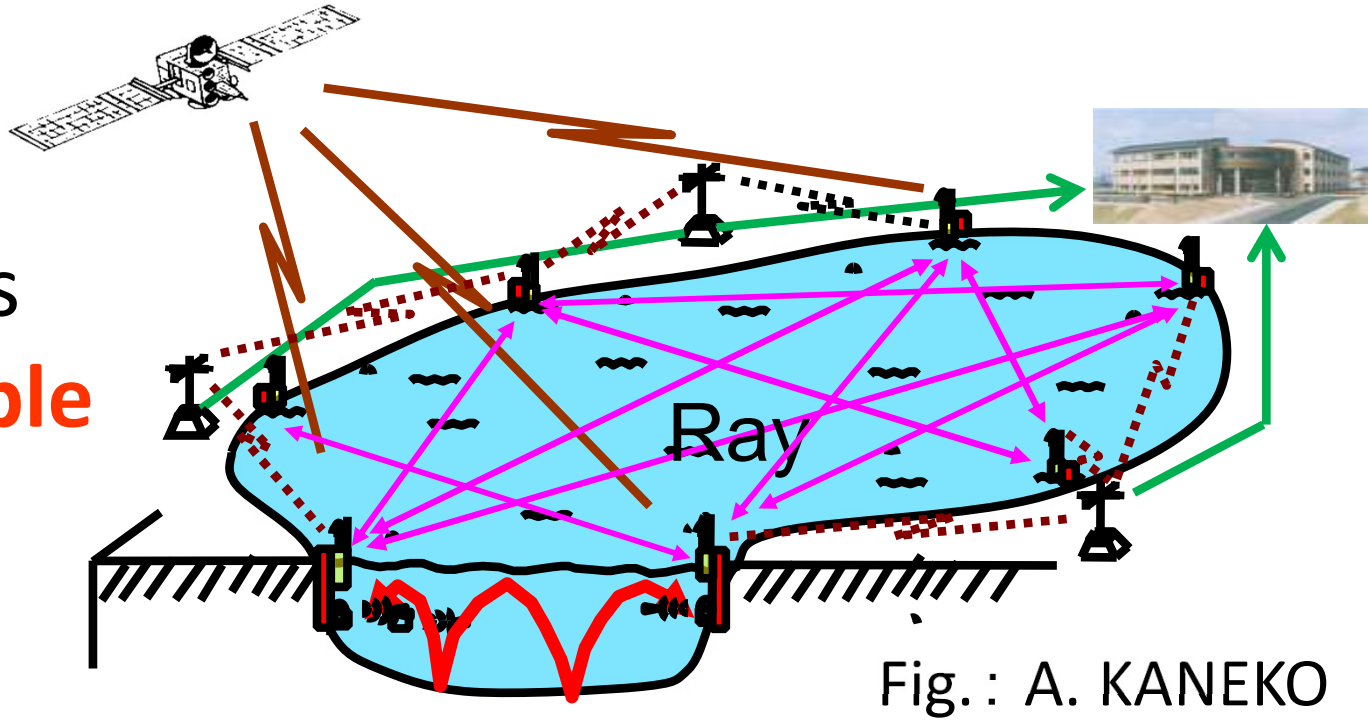


Fig.: A. KANEKO

aim to extend Zhu *et al*'s framework to **assimilate DTT** into hydrodynamic simulation of **lakes**.

Journal of Geophysical Research: Oceans

Published online 1 SEP 2

RESEARCH ARTICLE

10.1002/2017JC012715

Key Points:

- Coastal acoustic tomography data were assimilated into a triangular mesh ocean model for the first time
- Velocities obtained from assimilation agreed with ADCP data better than those from inversion or simulation
- Assimilation with a triangular mesh fits complex coastlines well and enables reasonable circulation calculations

Correspondence to:
X.-H. Zhu,
xhzhu@sio.org.cn

Assimilation of coastal acoustic tomography data using an unstructured triangular grid ocean model for water with complex coastlines and islands

Ze-Nan Zhu[1,2], Xiao-Hua Zhu[1,2], Xinyu Guo[3], Xiaopeng Fan[1], and Chuanzheng Zhang[1]

[1]State Key Laboratory of Satellite Ocean Environment Dynamics, Second Institute of Oceanography, State Oceanic Administration, Hangzhou, China, [2]Ocean College, Zhejiang University, Zhoushan, China, [3]Center for Marine Environmental Study, Ehime University, Matsuyama, Japan

Abstract For the first time, we present the application of an unstructured triangular grid to the Finite-Volume Community Ocean Model using the ensemble Kalman filter scheme, to assimilate coastal acoustic tomography (CAT) data. The fine horizontal and vertical current field structures around the island inside the observation region were both reproduced well. The assimilated depth-averaged velocities had better agreement with the independent acoustic Doppler current profiler (ADCP) data than the velocities obtained by inversion and simulation. The root-mean-square difference (RMSD) between depth-averaged

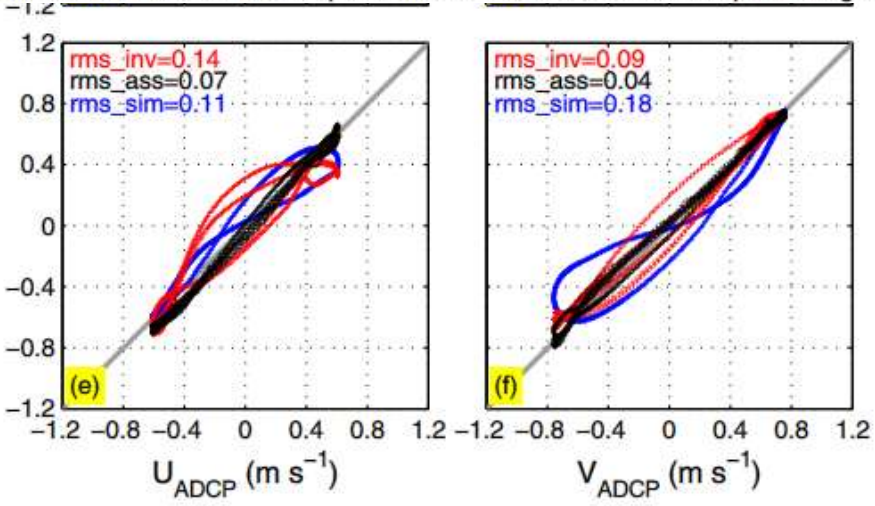


Figure 7. Scatter plots of (left) eastward and (right) northward velocity components with respect to ADCP at stations (top) A and (bottom) A3. The RMSDs between the ADCP and the inversion, assimilation, and simulation are shown in the top left of (in m s^{-1}).

lack of tides in lakes makes **our task substantially more difficult**, because of

1) **weaker currents** (~15% tidal)
2) **stronger stratification** of the density, thence more strongly 3D current fields

in lakes *vs.* tidal seas.

Prior CAT in lakes

- **Maximal range about 500 m**
- DTT done with moving ship by Xu et al ‘23
- Several examples of vertical slice inversion of temperatures, with 5 rays identified (group of H. Huang)
- Carrier freq. $\geqq$ 30 kHz

Electronics Manufactured by Marino Tomography LLC (A. Kaneko)



UBLOX timekeeping

5 kHz carrier

M11 * 6 rpt (9 repeats for ‘21)

Q = 3 cycles/bit

10’ ping intervals,
“round-robin” emit/receive

http://www.marinotomography.com/cats.html

Toroidal TR heights 2.5 m above bottom

Westward transducer (TR) for all data shown today: Fixed to water intake at Bottom Depth (BD) = 9 m

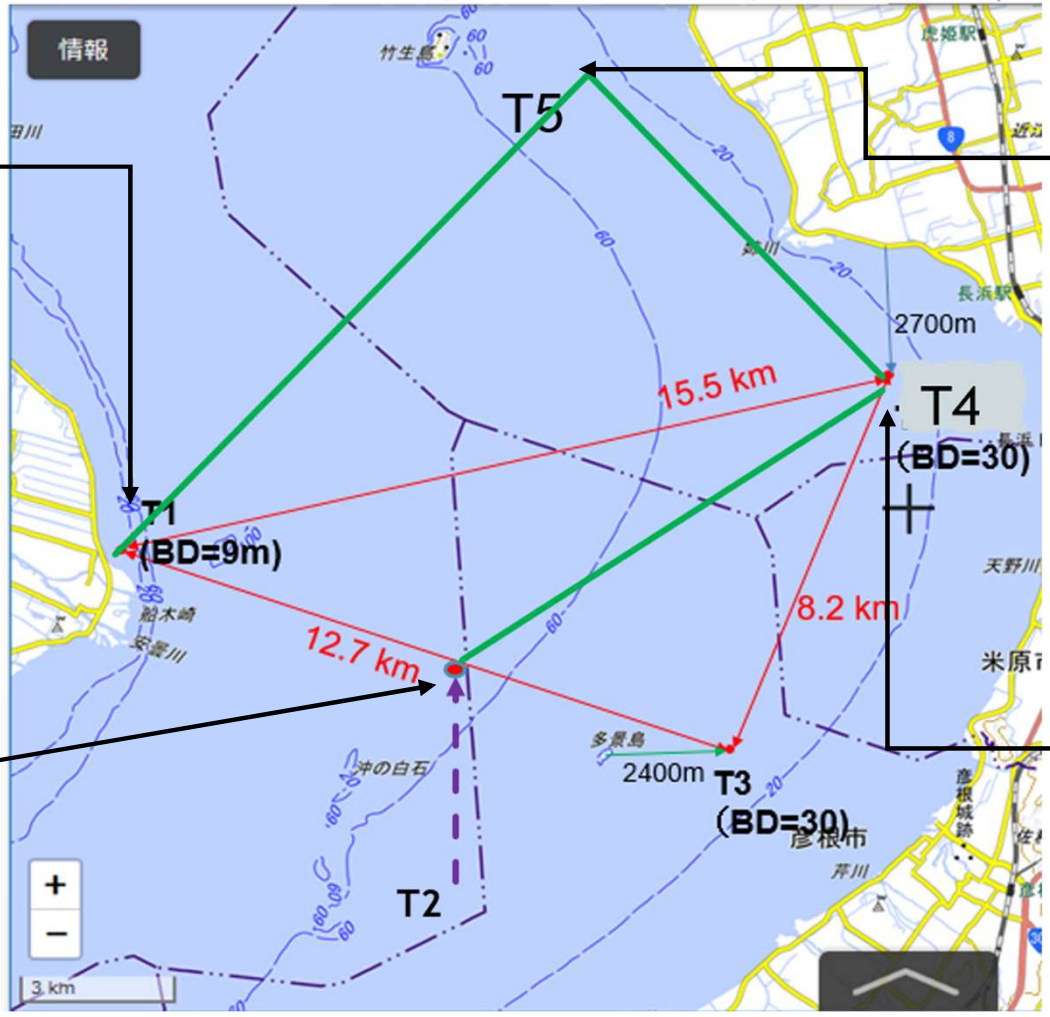


Tonpilz “directional” TR
at depth 4.5 m



Autumn ‘18 (mostly Nov.); up to 5 TR







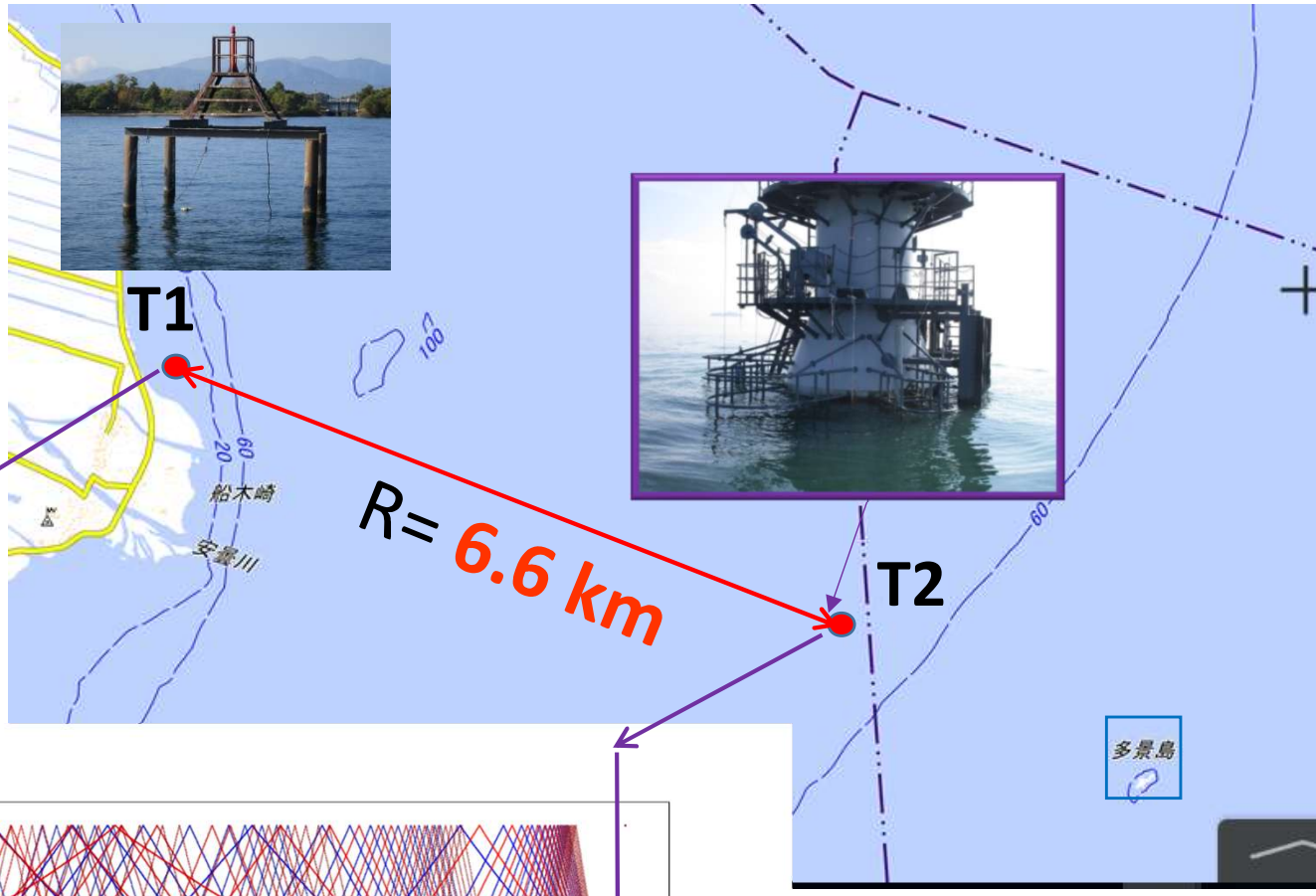




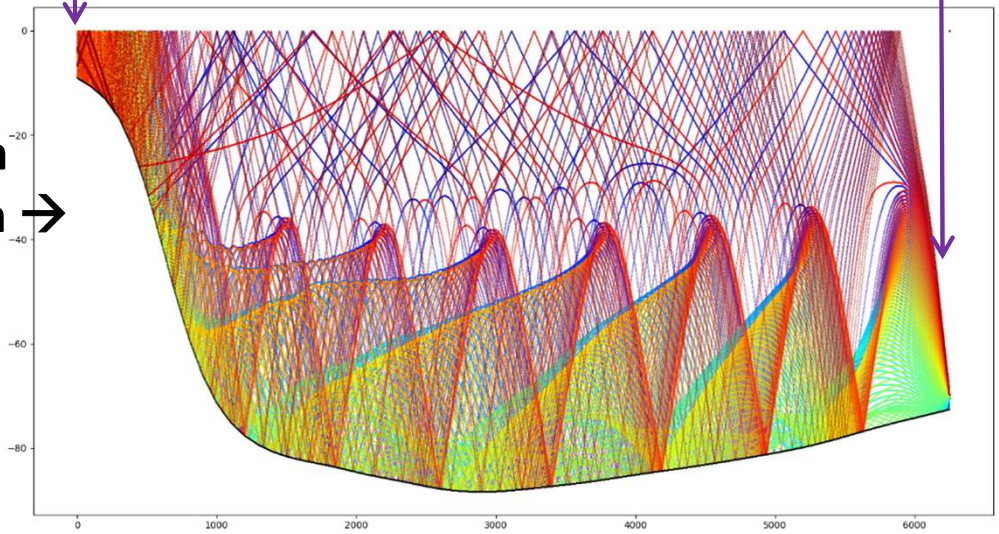
T2 – T5; moored, BD 30~68 m, TR 2.5 m above bottom

“round-robin” emit/receive in 10’ cycle

Sectional Bathymetry



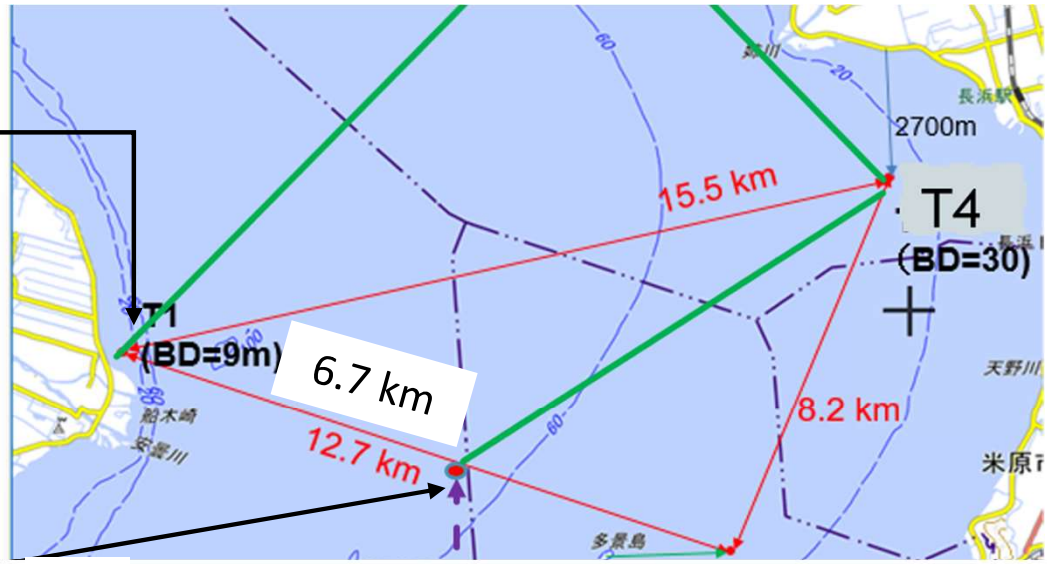
Axial TR 4.5 m above bottom →



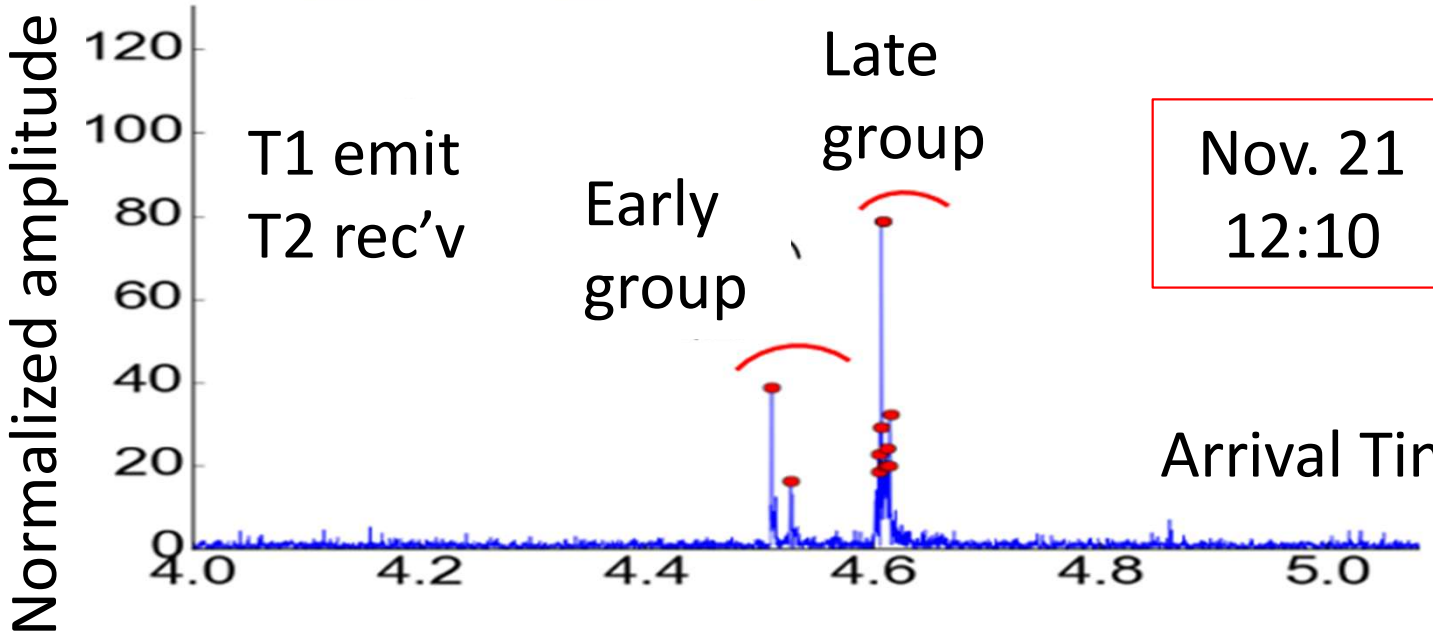
← Toroidal TR 2.5 m above bottom







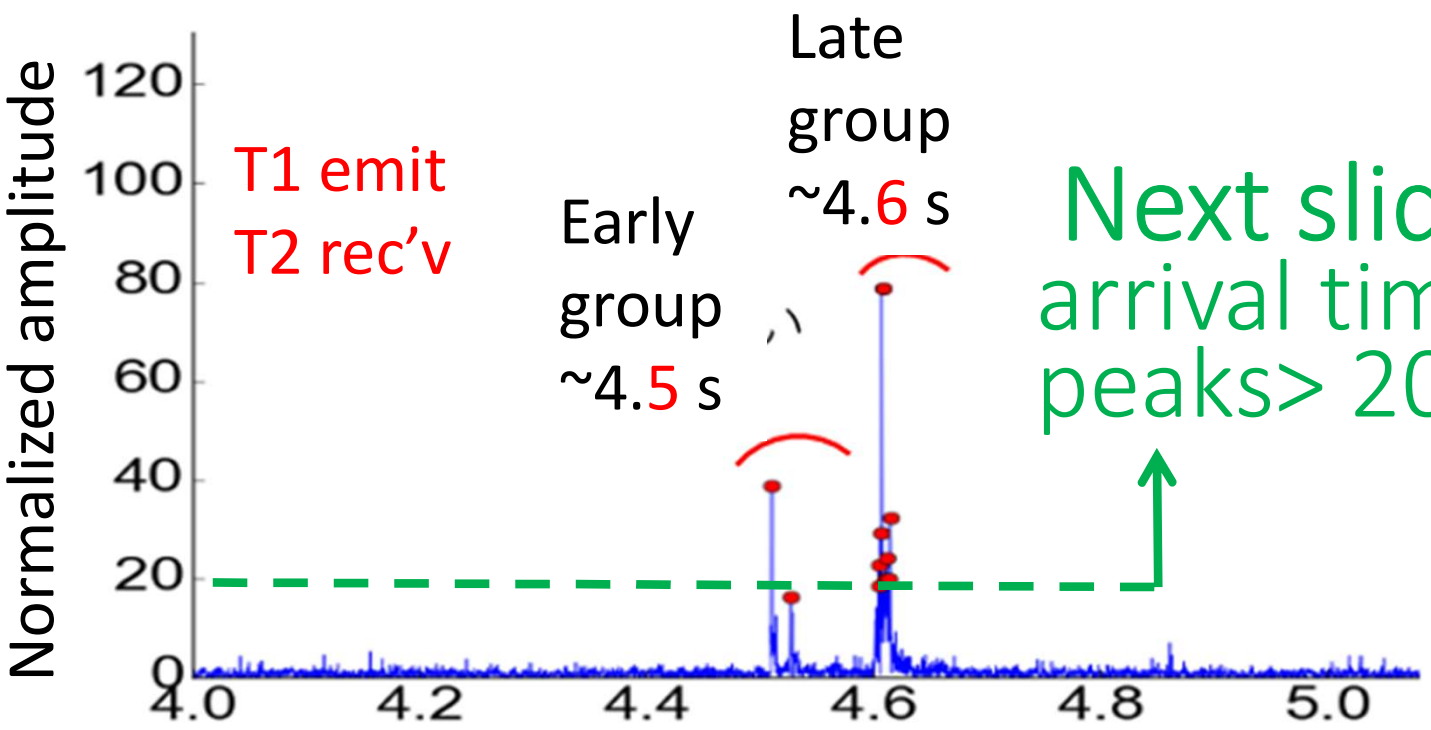
Nov. ’18; frequent double peak patterns

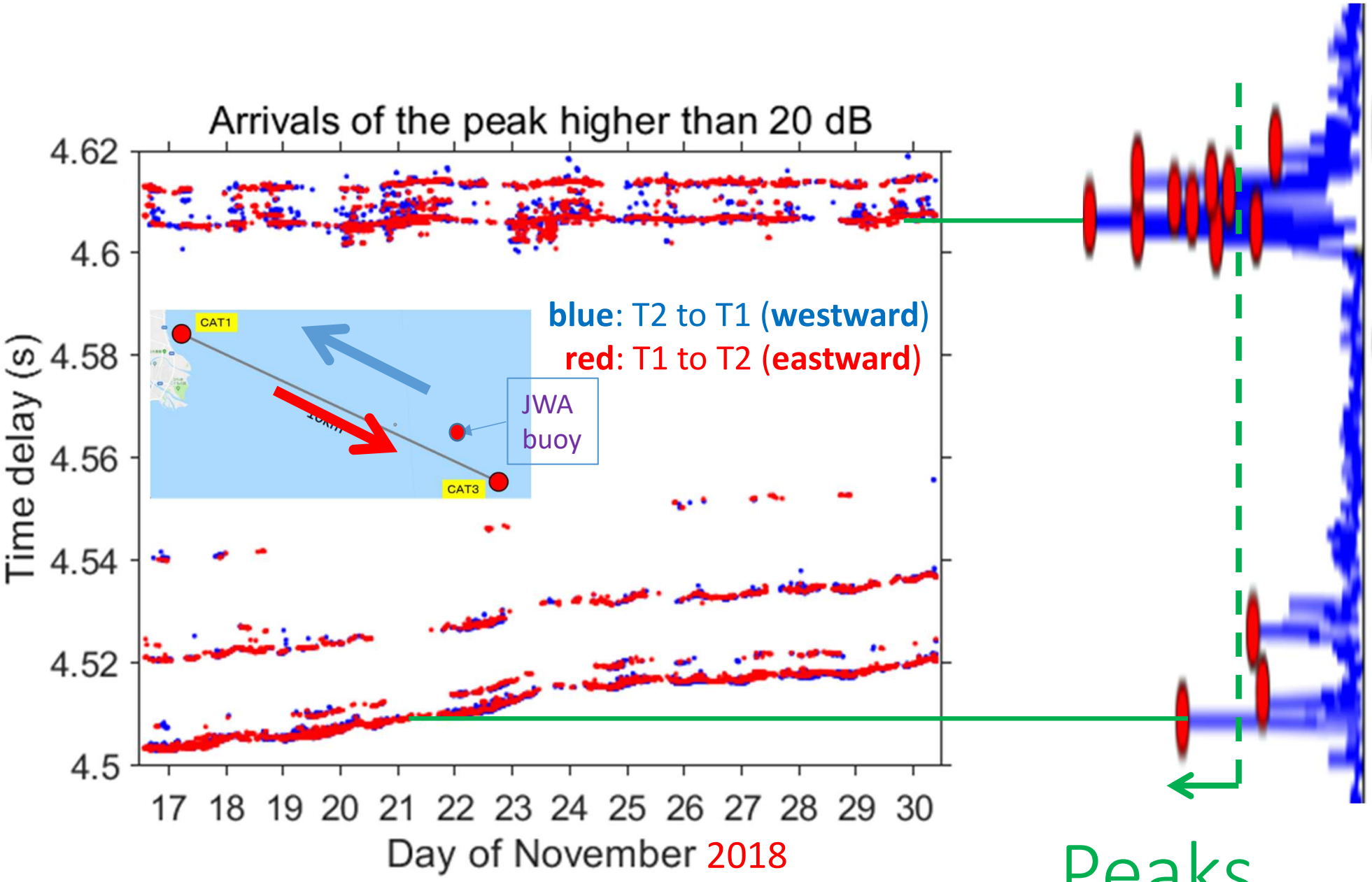


Nov. 21
12:10

next slides show: early arrivals thru sfc layer
late arrivals thru deep water

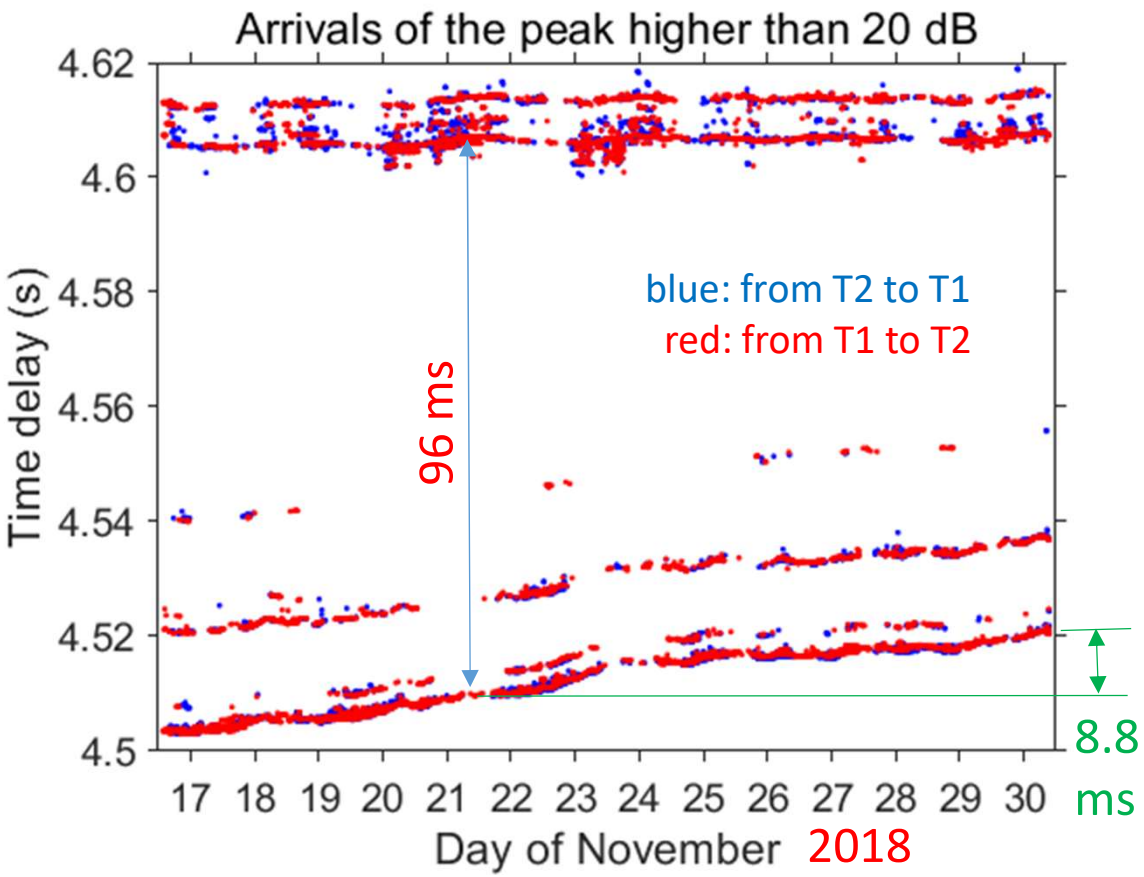
Nov. ’18; frequent double peak patterns

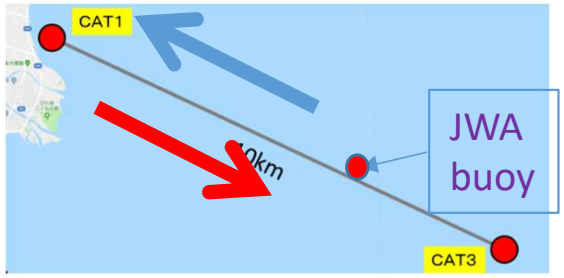



Arrivals of the peak higher than 20 dB
Time delay (s)
4.62
4.6
4.58
4.56
4.54
4.52
4.5
17 18 19 20 21 22 23 24 25 26 27 28 29 30
Day of November 2018
CAT1
CAT3
JWA
buoy
blue: T2 to T1 (westward)
red: T1 to T2 (eastward)

Peaks
> 20dB

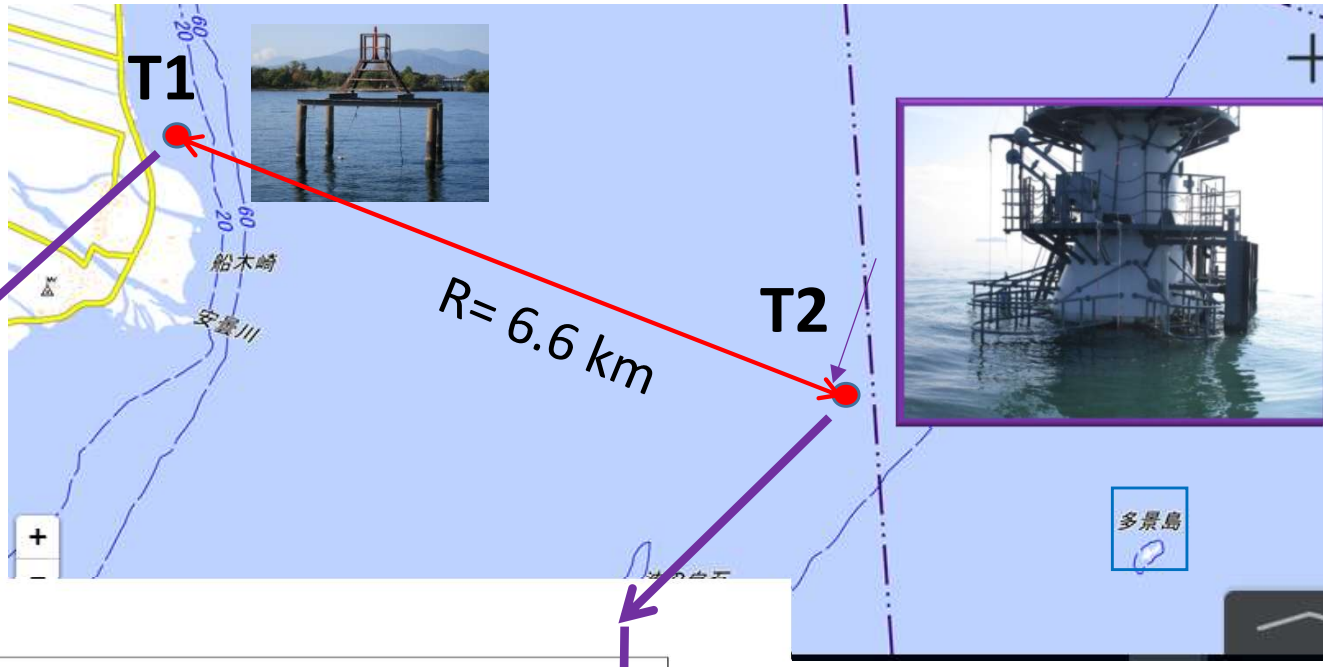
Hypothesis: surface waveguide acting?
(at least in autumn)

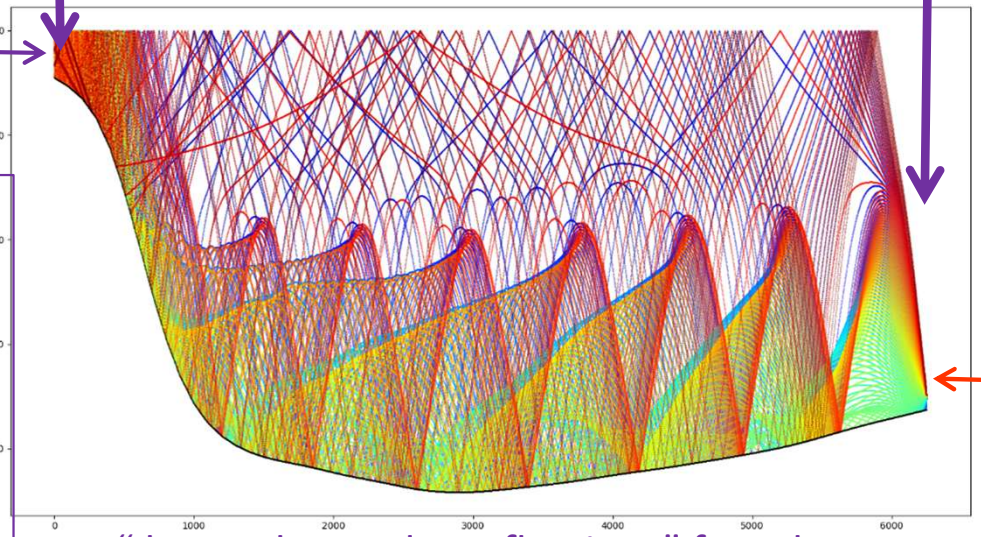




- Between T1 and T2 (R = 6.6 km) there were two arrival groups (ca. 4.5 and 4.6 s).
- **The arrival times of the first group get slower (i.e., average sound speed decreases), but not those of the later arrival group**
- Temps @T2 on Nov 21, namely 16.4 C @d=10m, 7.9 C @d= 60m, explain the observed difference of first arrivals in each group, 96 ms, to within 1 ms!
- Surface layer cooling observed between Nov 21 and 29 (16.4 -> 14.6 C) explains observed slowing of 8.8 ms

evidence for two "routes" from acoustic ray-tracing (RT) simulations (*time-matched (T,u,v) from 3D hydro simulations*)



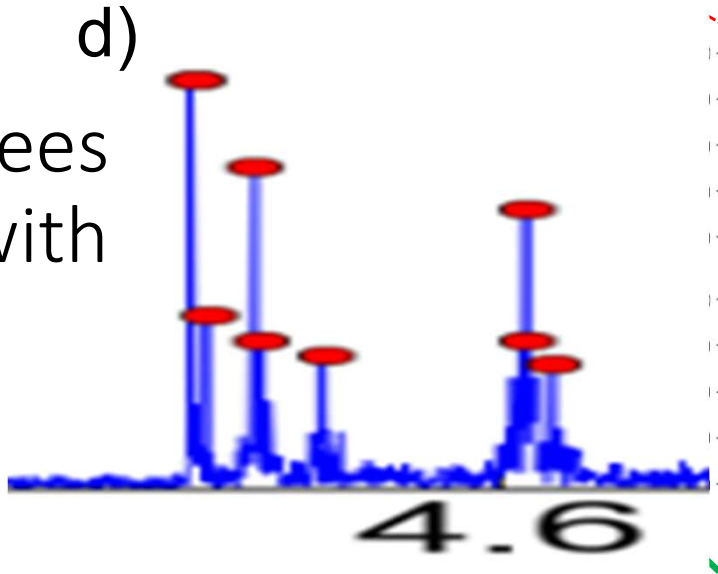


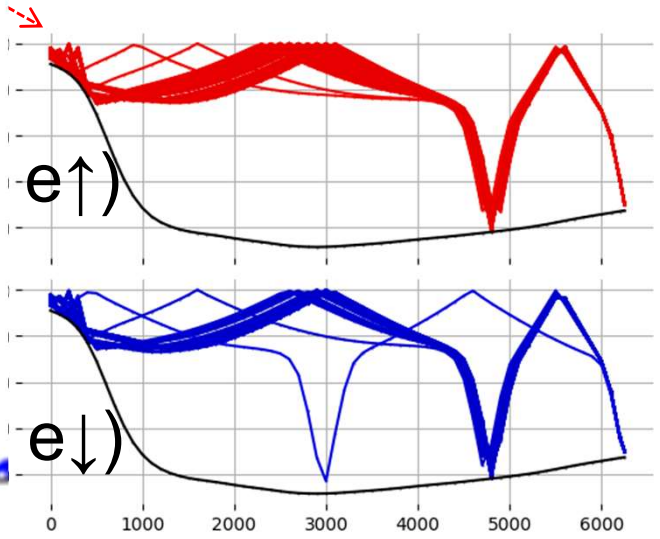
"damped specular reflections" from bottom

Retain only those rays that "hit" T1 (4.5 m above bottom at water intake) → **synthesize received waveform**

Trace **200K** virtual rays **emitted westward** from T2 (2.5 m above bottom near JWA buoy

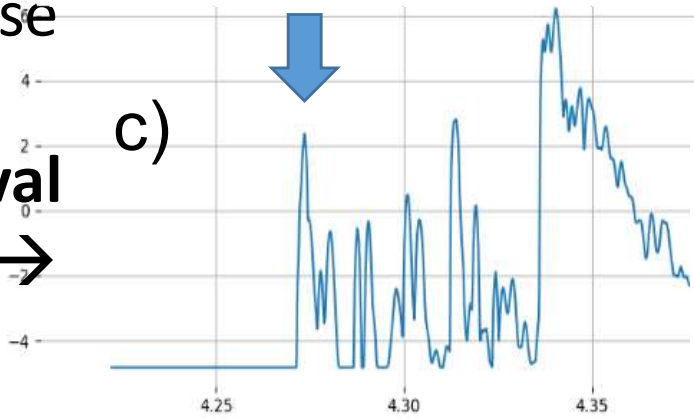
Observed waveform agrees qualitatively with synthetic →

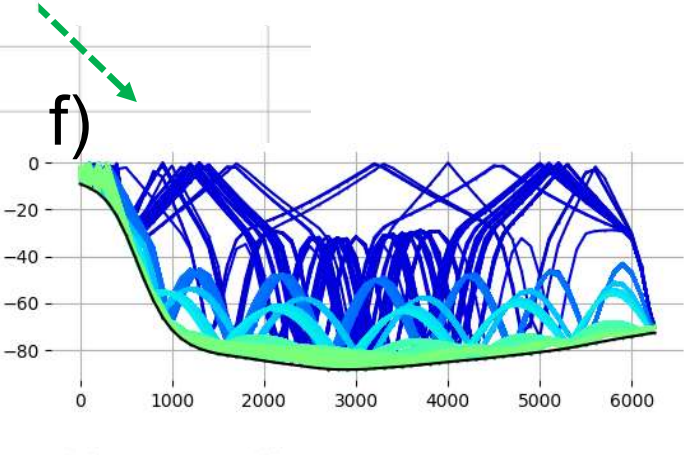




Rays forming earliest peak

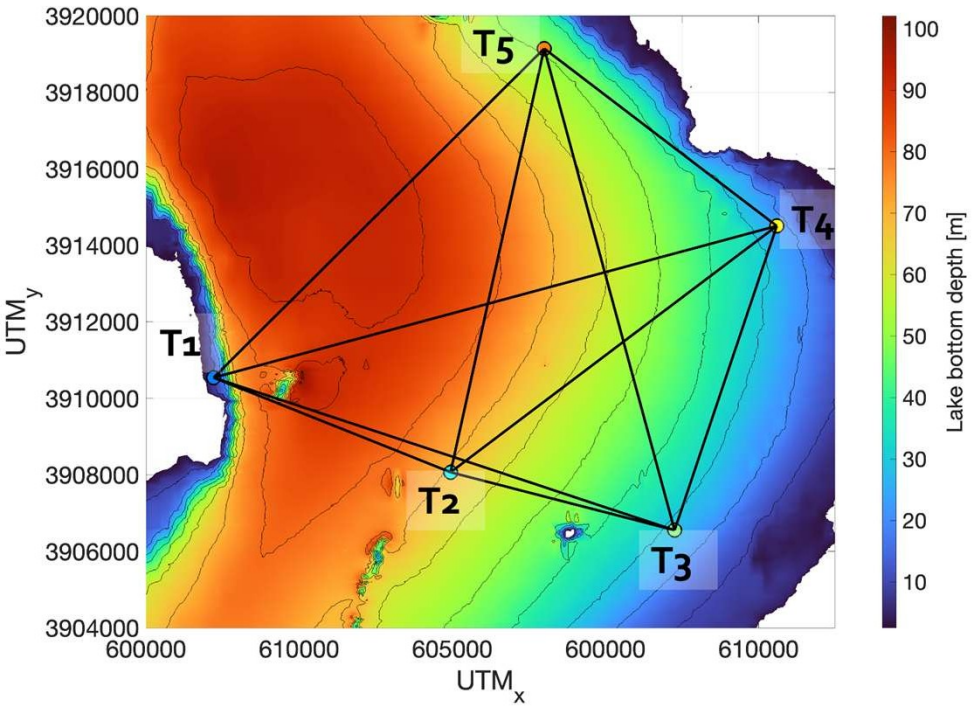
Convolve impulse responses to **synthesize arrival waveforms** →





Rays forming later main peak

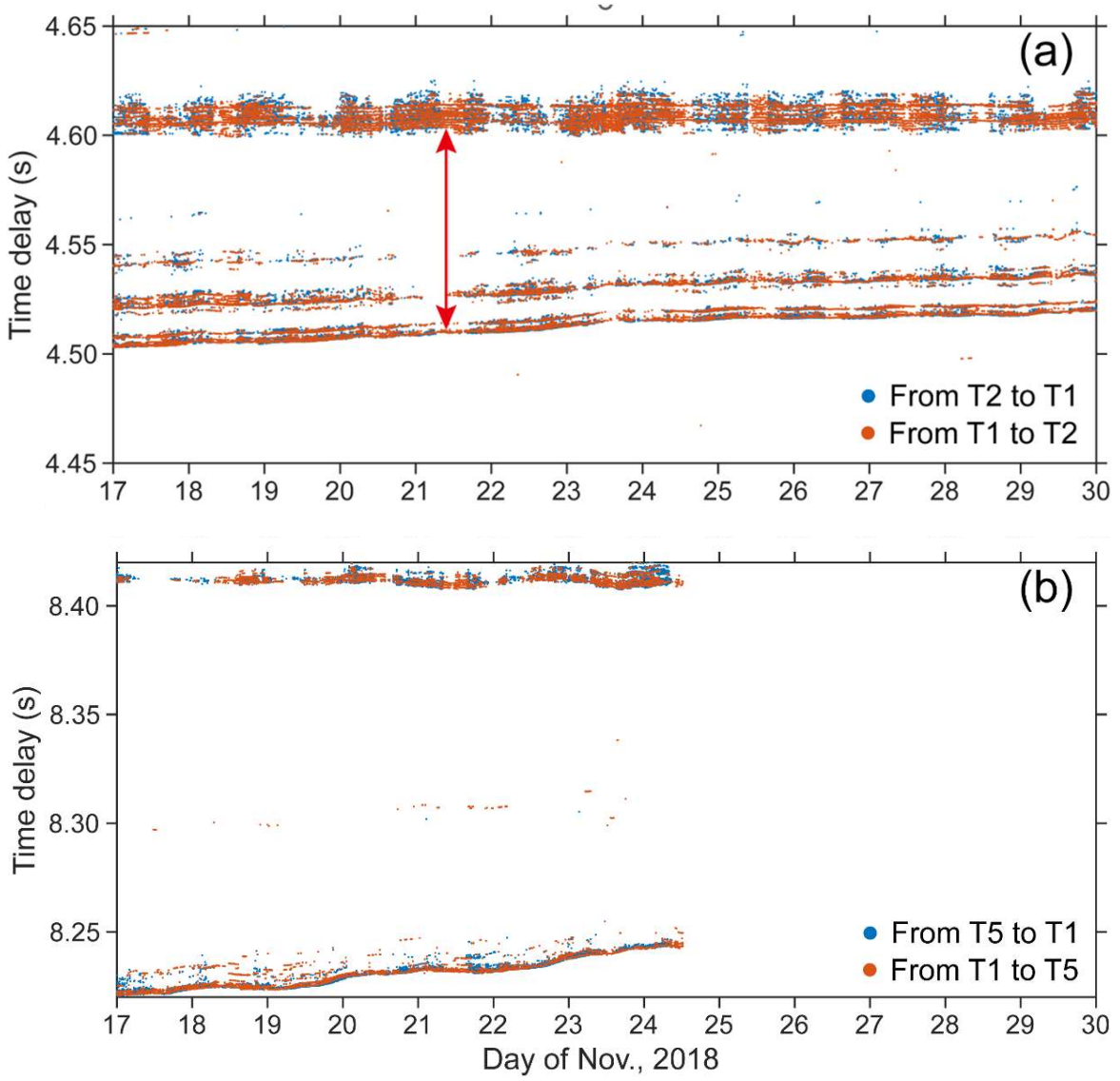
These two arrival groups were found at two other transects



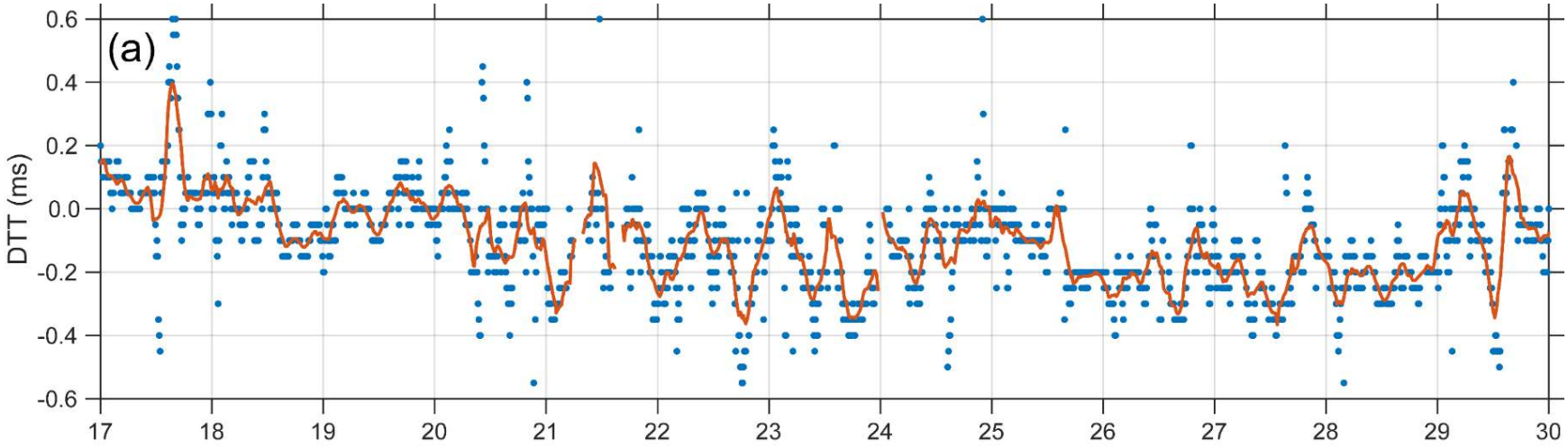
Stn.	T1	T2	T3	T4	T5
T1		6595	12685	15237	12190
T2	17-30*		6097	10560	11147
T3	17-24	16-24		8389	13044
T4	22-30	22-30	22-24		7644
T5	17-24*	22-24*	17-24	21-24	

Reciprocal arrival times versus JST datetime, for (a) **T1-T2**, (b) **T1-T5.**

dots where Amp>14dB



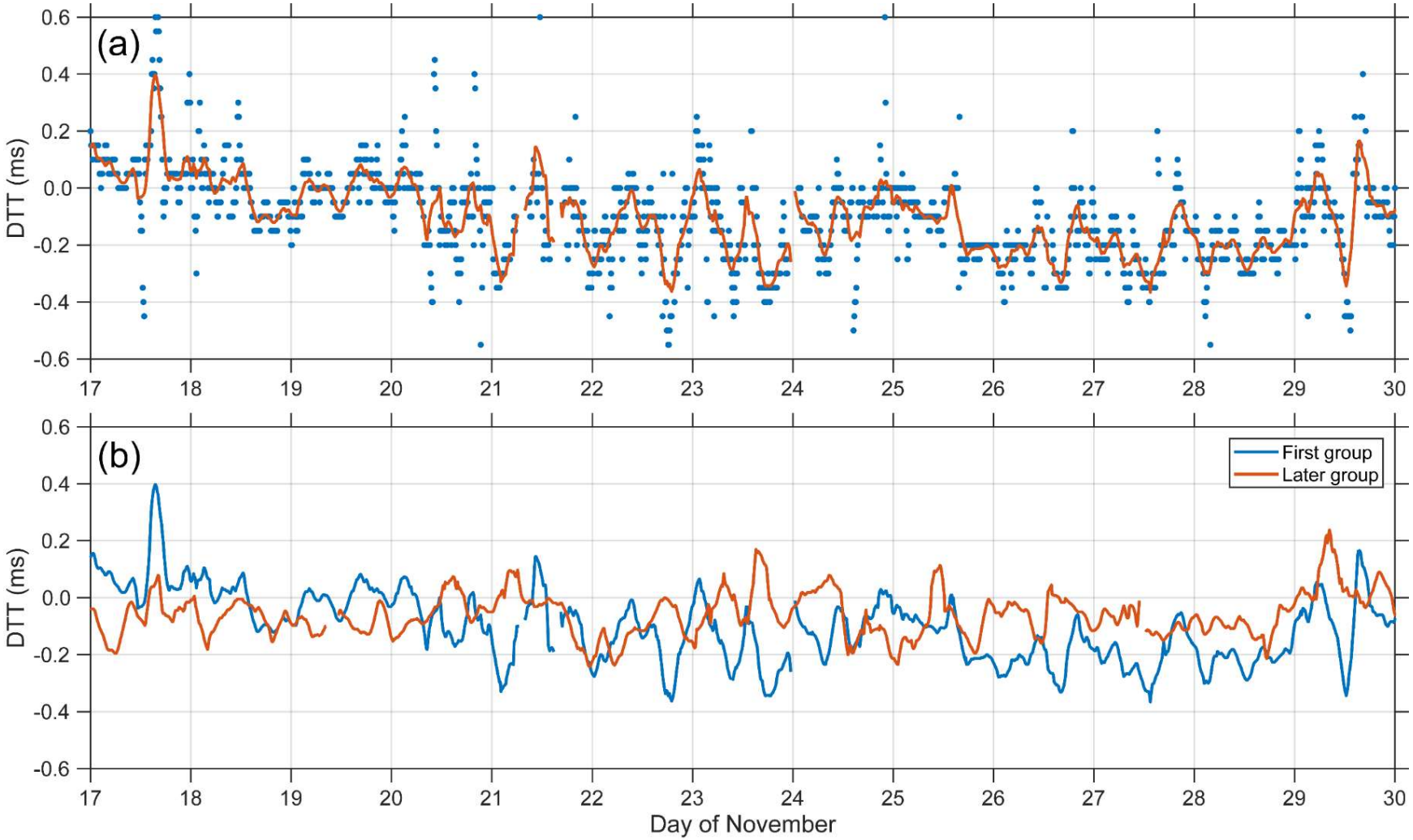
differential travel time T1 – T2



Timeseries of DTT from time-averaged (n=19, three hours) reciprocal arrival signals between T1 and T2. (Positive DTT → path-averaged current from T1 to T2),

(a) results for the first arrival group, where the dots denote individual DTT with 2X subsampling , and the continuous curve results from a further averaging of those dots over a three hour window, when 10 or more valid values are available (out of a potential 19).

differential travel time T1 – T2

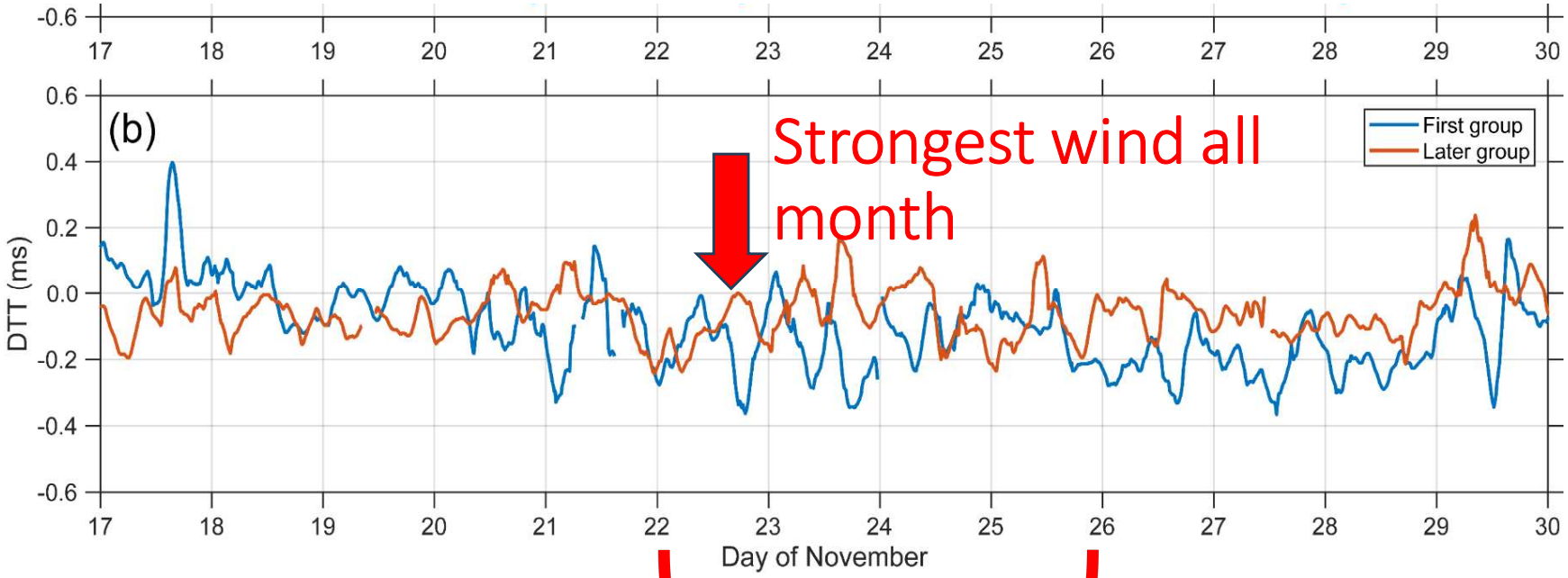


Timeseries of DTT from time-averaged (n=19, three hours) reciprocal arrival signals between T1 and T2. (Positive DTT → path-averaged current from T1 to T2),

(a) results for the first arrival group, where the dots denote individual DTT, and the continuous curve results from a further averaging of those dots over a three hour window, when 10 or more valid values are available (out of a potential 19).

(b) The time-averaged curve for the **early group from (a) is replotted in blue**, as superposed with the corresponding time-averaged DTT. **from the later arrival group in orange**

differential travel time T1 – T2



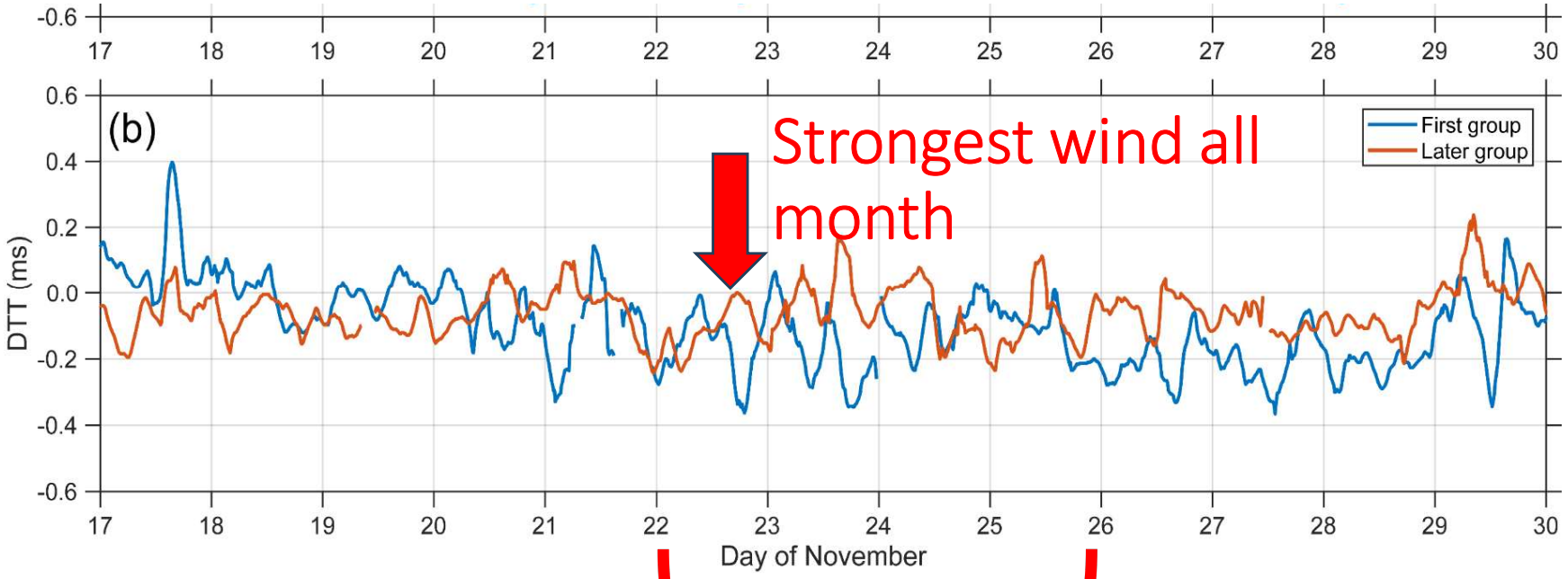
Timeseries of DTT from time-averaged (n=19, three hours) reciprocal arrival signals between T1 and T2. (Positive DTT → path-averaged current from T1 to T2),

(b) The 3-hr time-averaged curve for the **early group from (a) is replotted in blue**, as superposed with the corresponding time-averaged DTT. **from the later arrival group in orange**

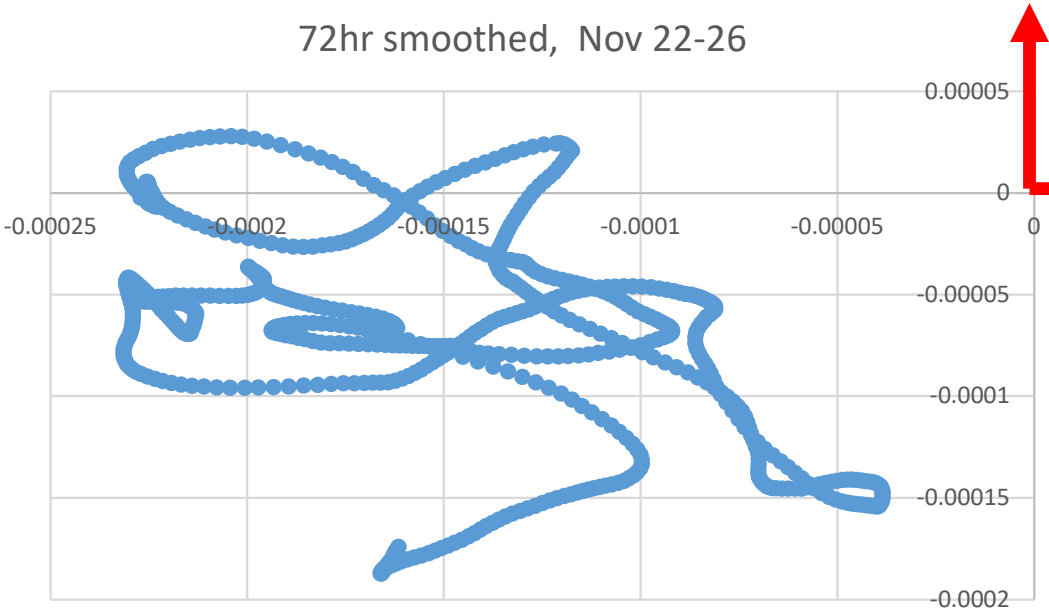
Applying additional smoothing to these DTT timeseries by a 72-hour tophat filter, we compute a correlation coefficient of -0.495 for the interval Nov 22-26.

Also, consistent bias (?flow T2 → T1?)

differential travel time T1 – T2



DTT*late*



DTT *early*

Applying additional 72-hr running avg to these DTT timeseries we compute a correlation coefficient of -0.495 for the interval Nov 22-26.

Also, consistent bias (flow T2 → T1)

For data assimilation, will need a measurement model for Differential Travel Time "DTT"

State estimate from SUNTANS hydrodynamic model

→

Model acoustic propagation **(RAM) ← currents w/ "Effective Sound-Speed Approximation"**

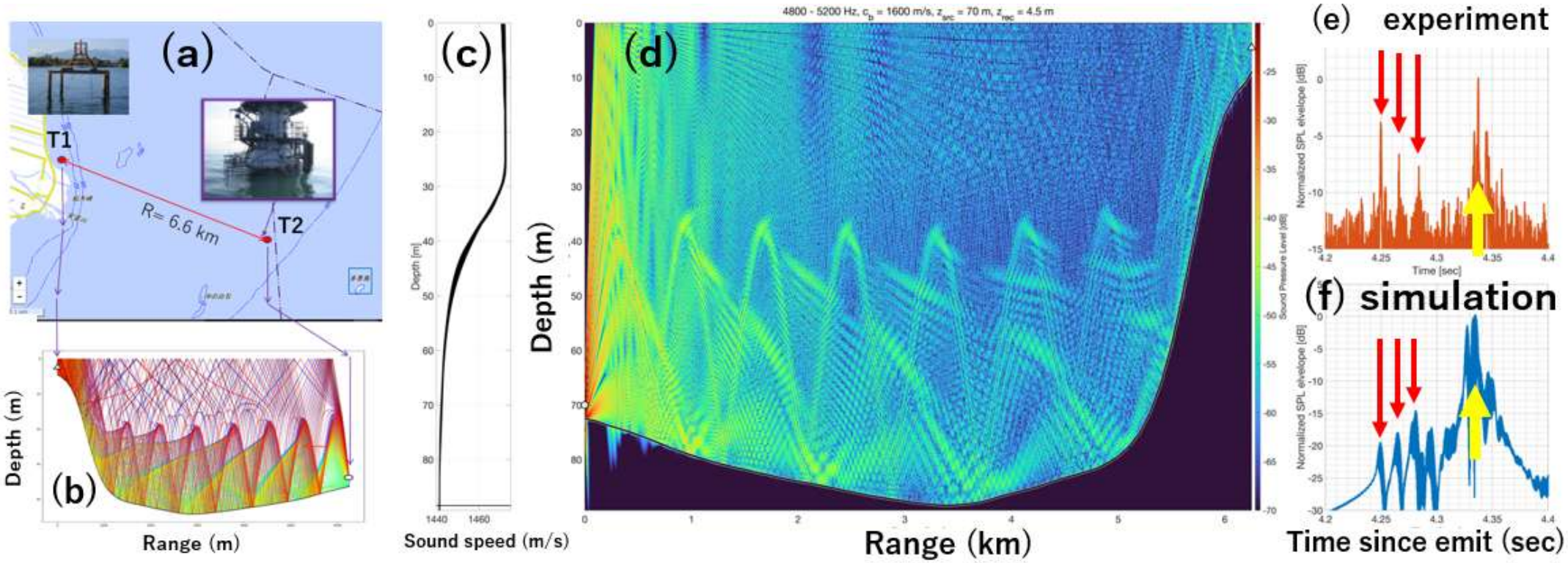
→

Model DTT

→

Improve estimate of current state

PE/RAM simulations yield arrival times better than RT



We now exploit RAM's capability to **simulate DTT**

*Important: "assumed sediment properties for **gas-free silty clay**". **Other sediment props give rather different arrival times**! Especially, methane gas bubble concentration in lakebed is an important and "tricky" factor*

Simulate Differential Travel Time “DTT”

State estimate from (T-nudged) SUNTANS hydrodynamic model

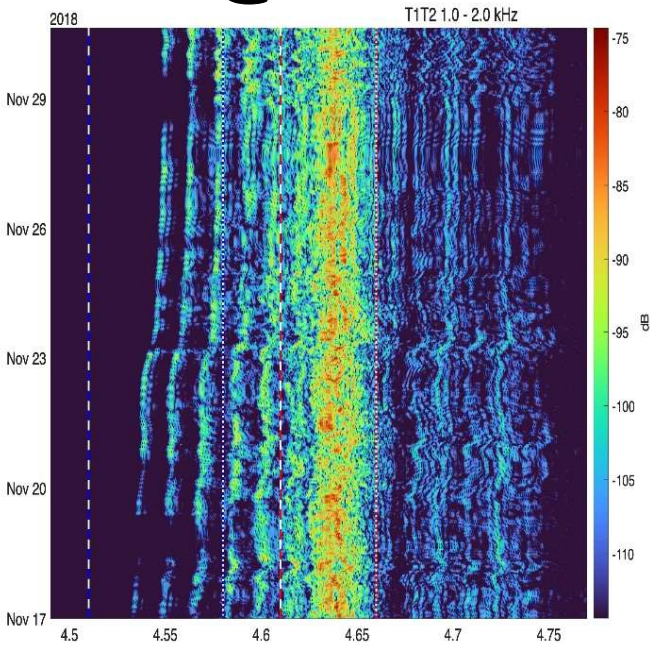
→

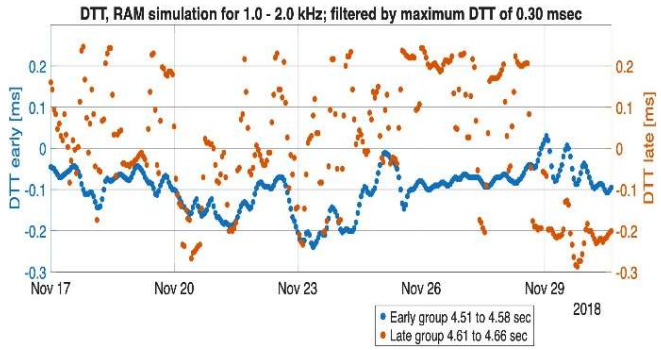
Model acoustic propagation **(RAM)**

→

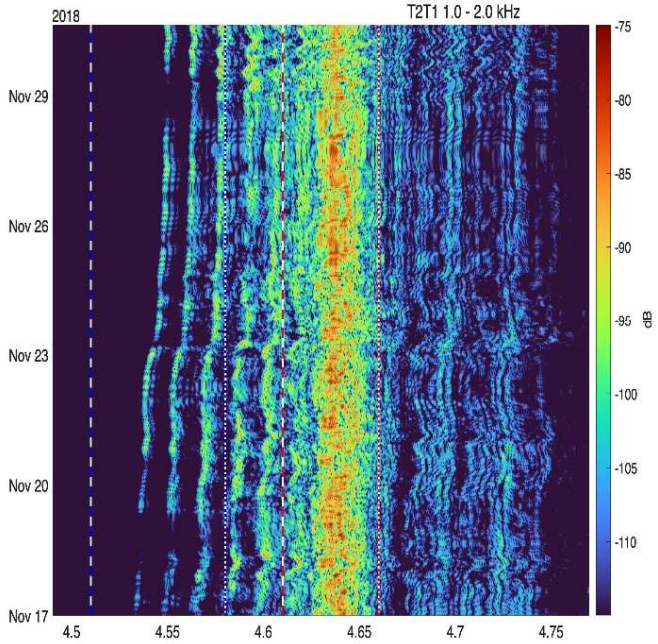
Model DTT

DTT@T1--> T2



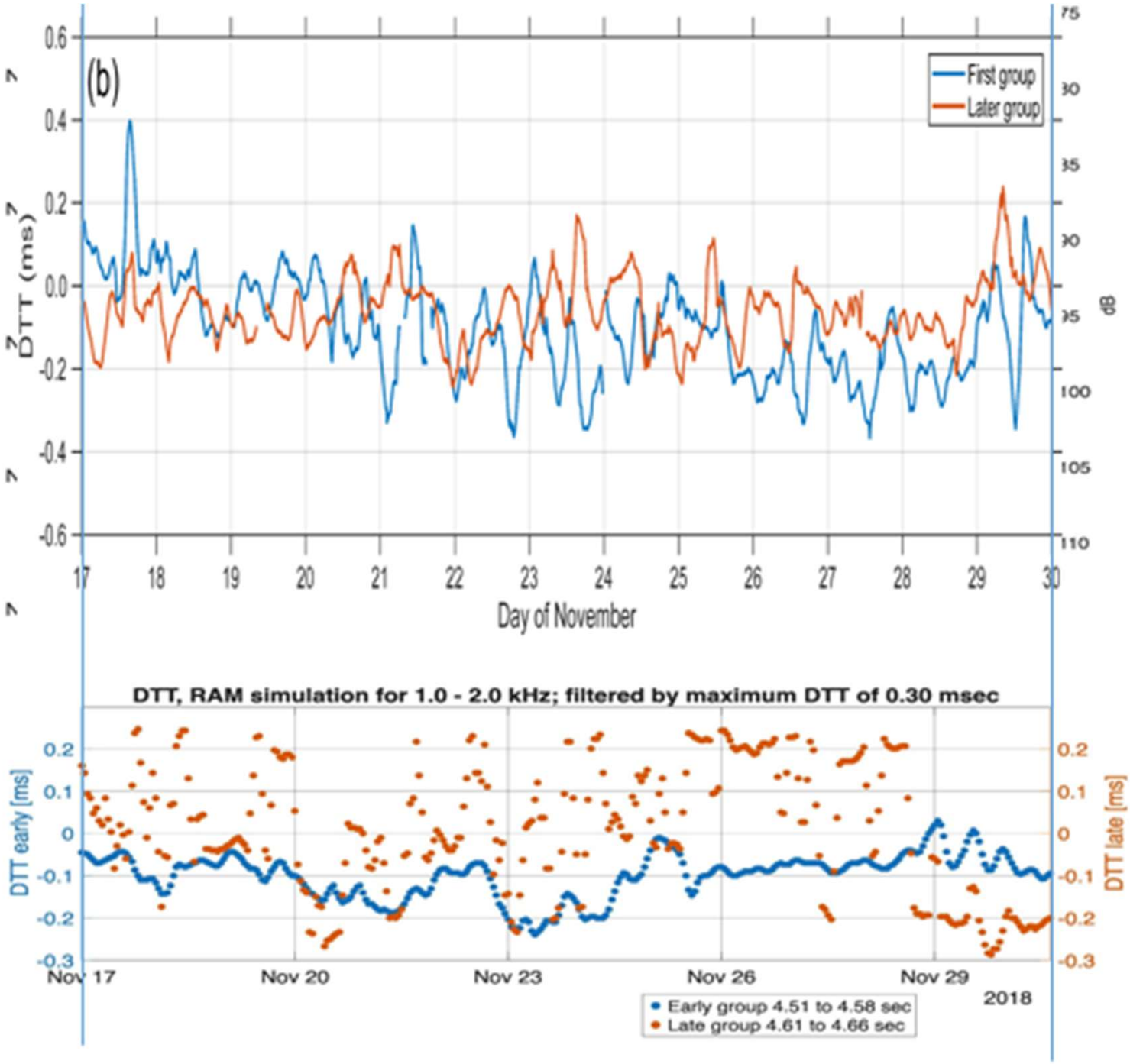


T2--> T1



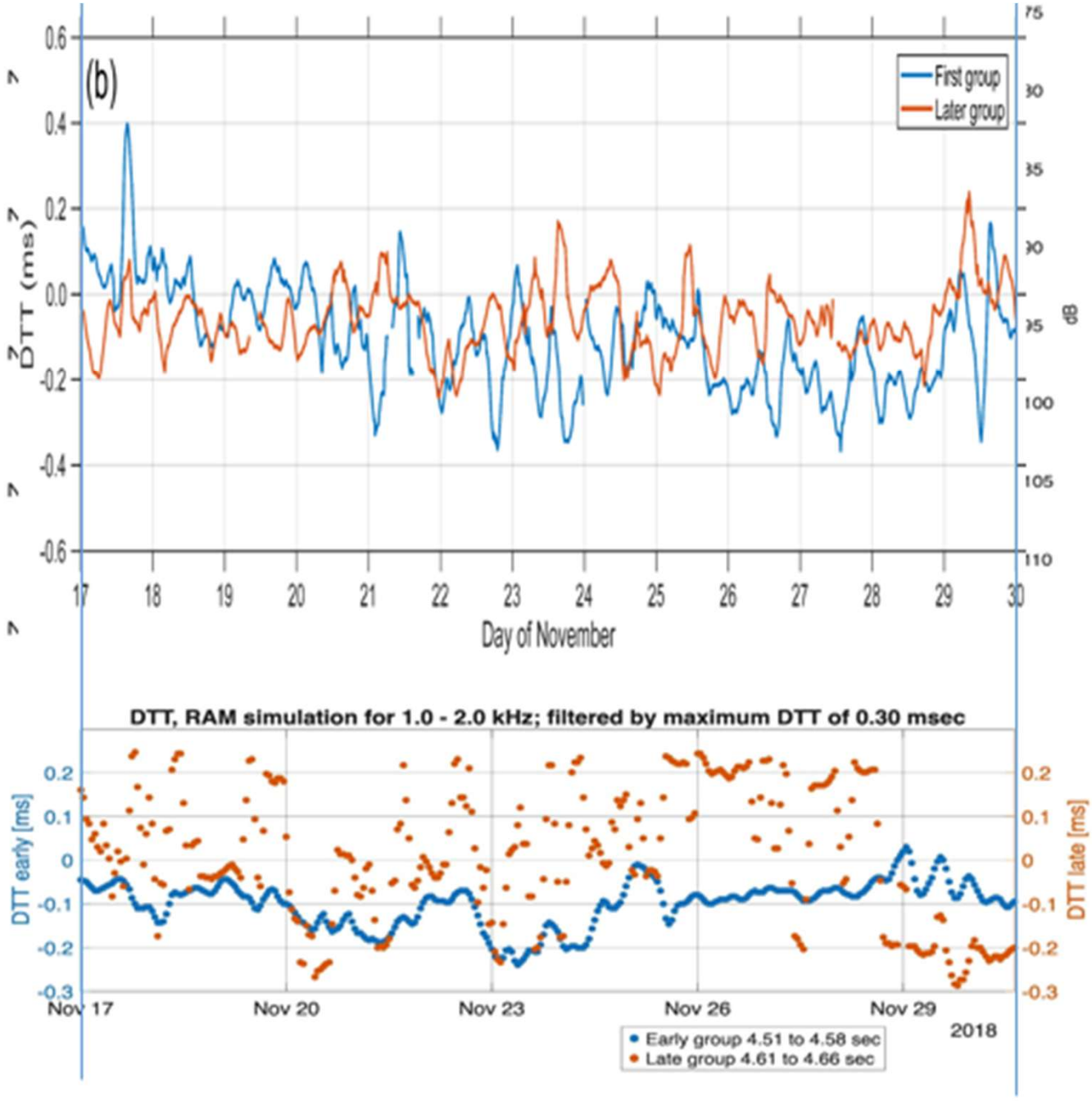
Obs DTT:

Simulated Differential Travel Time "DTT" →



Obs DTT" →

Simulated Differential Travel Time "DTT" of early arrivals → (<-> sfc current) yields a similar negative bias



To "globally" exploit phase information, we have attempted the **first** application of Godin *et al.'s* (1996) **matched nonreciprocity method** to real field data.

This method estimates effective currents by **minimizing three functionals** that quantify the discrepancy between the experimentally observed and theoretically predicted nonreciprocity of 1) sound intensity, F_a, 2) acoustic field **phase**, F_p, and 3) complex acoustic field, F_c.

Numerical modeling was performed using RAM (wide-angle parabolic equation), incorporating realistic bottom topography and spatially variable (numerically simulated) temperatures in the lake.

(

WHY "global"? **Traditional current tomography methods based on DTT require a sufficient number of resolved and identified pairs of counter-propagating eigenrays.**

But in shallow water, rays may not be sufficiently resolved in time. At best, their identification is uncertain due to the poorly known bottom impedance and topography [Uzhansky et al 2024].

)

$$F_a = 2\frac{\langle |p_e^{(+)}| - |p_e^{(-)}| - |p_t^{(+)}| + |p_t^{(-)}| \rangle}{\langle |p_e^{(+)}| - |p_e^{(-)}| \rangle + \langle |p_t^{(+)}| + |p_t^{(-)}| \rangle} \quad (1)$$

phase

F_p

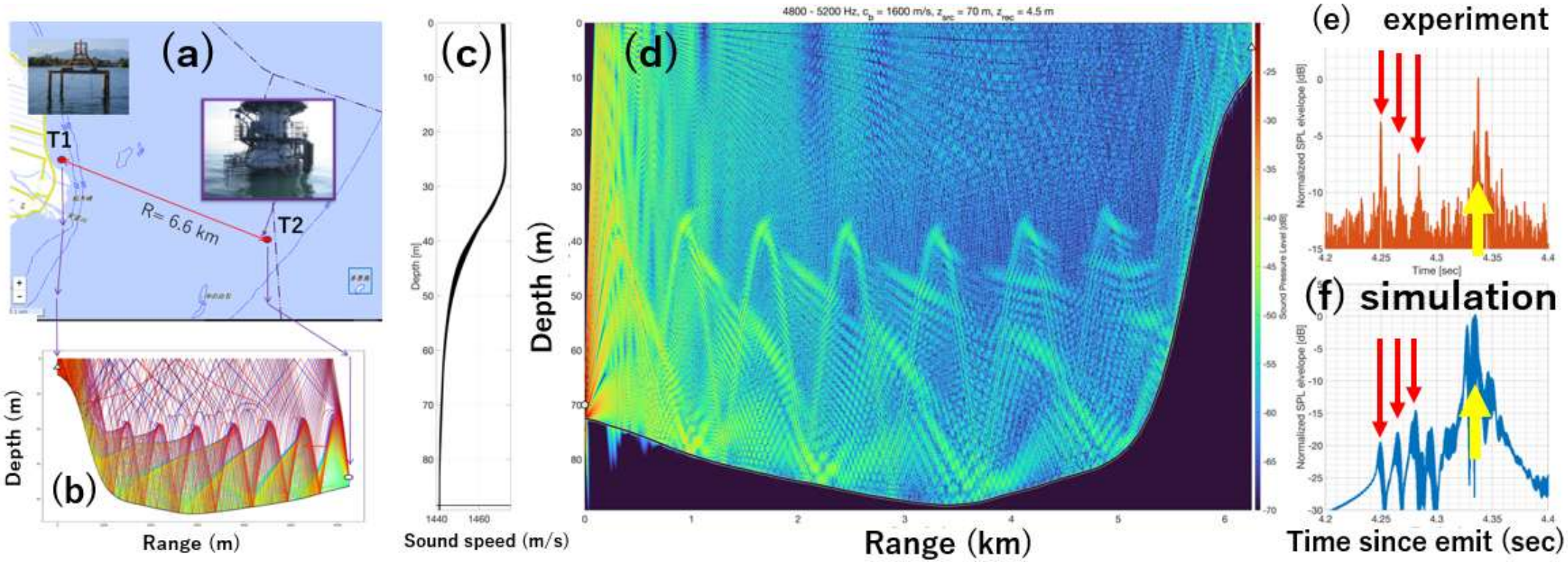
"**e**": experiment "**t**": theory (RAM)

$$= 2\frac{\langle \arg\left(\frac{p_e^{(+)} p_t^{(-)}}{p_e^{(-)} p_t^{(+)}}\right) \left| p_e^{(+)} p_e^{(-)} p_t^{(+)} p_t^{(-)} \right|^{1/4} \rangle}{\langle \left| p_e^{(+)} p_e^{(-)} \right|^{1/2} \rangle + \langle \left| p_t^{(+)} p_t^{(-)} \right|^{1/2} \rangle} \quad (2)$$

$$F_c = 2\frac{\langle |p_e^{(+)} - p_e^{(-)} - p_t^{(+)} + p_t^{(-)}| \rangle}{\langle |p_e^{(+)} - p_e^{(-)}| \rangle + \langle |p_t^{(+)} - p_t^{(-)}| \rangle} \quad (3)$$

These functionals minimize the discrepancy between the measured and theoretically predicted non-reciprocities of (1) the sound intensity, (2) the field phase, and (3) the complex acoustic field. Here, $p^{(\pm)}$ is the complex sound pressure for signals propagating from T1 to T2 (+), and T2 to T1 (−), respectively, the subscripts t and e denote theoretical (simulated) and experimental data, and arg( ) denotes the argument of a complex number. The angular brackets denote mean-square values over the frequencies used, which in our case are 200, 300, 400, and 500 Hz.

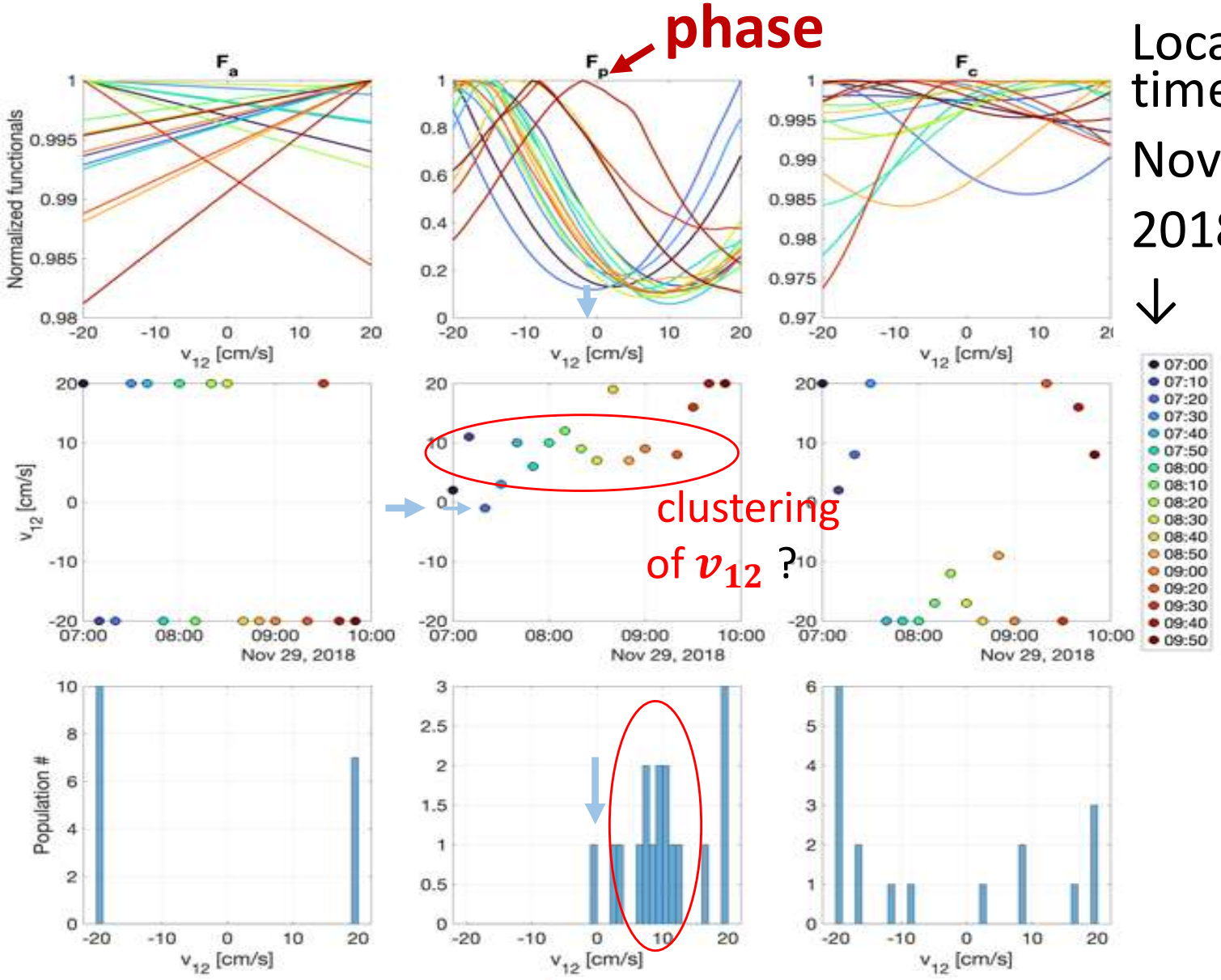
PE/RAM simulations yield arrival times better than RT



We now exploit RAM's capability to estimate functional F_p

Numerical modeling was performed using a wide-angle parabolic equation (RAM) incorporating realistic bottom topography and simulated spatially variable temperature profiles in the lake. Applied Effective Sound Speed Approximation, gas-free silty clay bottom

In this first attempt, **take current v_{12} spatially constant** (positive from T1 toward T2; bias not inconsistent with DTT/early and late at that time, but magnitude greater overall)



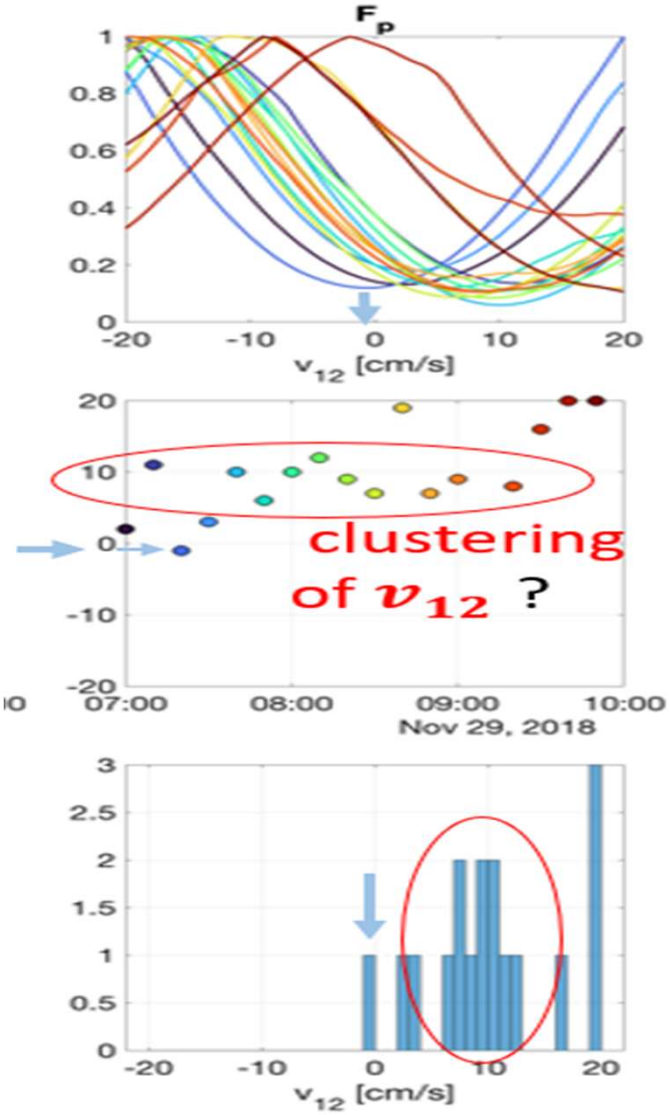
F_p ← **phase**

$$= 2\frac{\left\langle \arg\left(\frac{p_e^{(+)}p_t^{(-)}}{p_e^{(-)}p_t^{(+)}}\right)\left|p_e^{(+)}p_e^{(-)}p_t^{(+)}p_t^{(-)}\right|^{1/4}\right\rangle}{\left\langle\left|p_e^{(+)}p_e^{(-)}\right|^{1/2}\right\rangle+\left\langle\left|p_t^{(+)}p_t^{(-)}\right|^{1/2}\right\rangle}$$

Summary : observed small but consistent **differential travel times (*DTT*)**. But estimation by DTT of path-averaged currents has been *difficult to validate with ground truth (esp. for late arrivals)*.

→ First application of Godin *et al.'s* (1996) **matched nonreciprocity method (MNM)** to field data. We have estimated averaged currents by **minimizing a functional** F_p that quantifies the discrepancy between the experimentally observed and theoretically predicted nonreciprocity of acoustic field **phase**.

The MNM methodology may **complement** DTT to estimate large-scale currents, in lakes and other shallow-water sites.



Next; benthic methane mapping !?

A paper describing most of these results will soon appear in

IEEE J. Oceanic Engineering

Email jwells@se.ritsumei.ac.jp

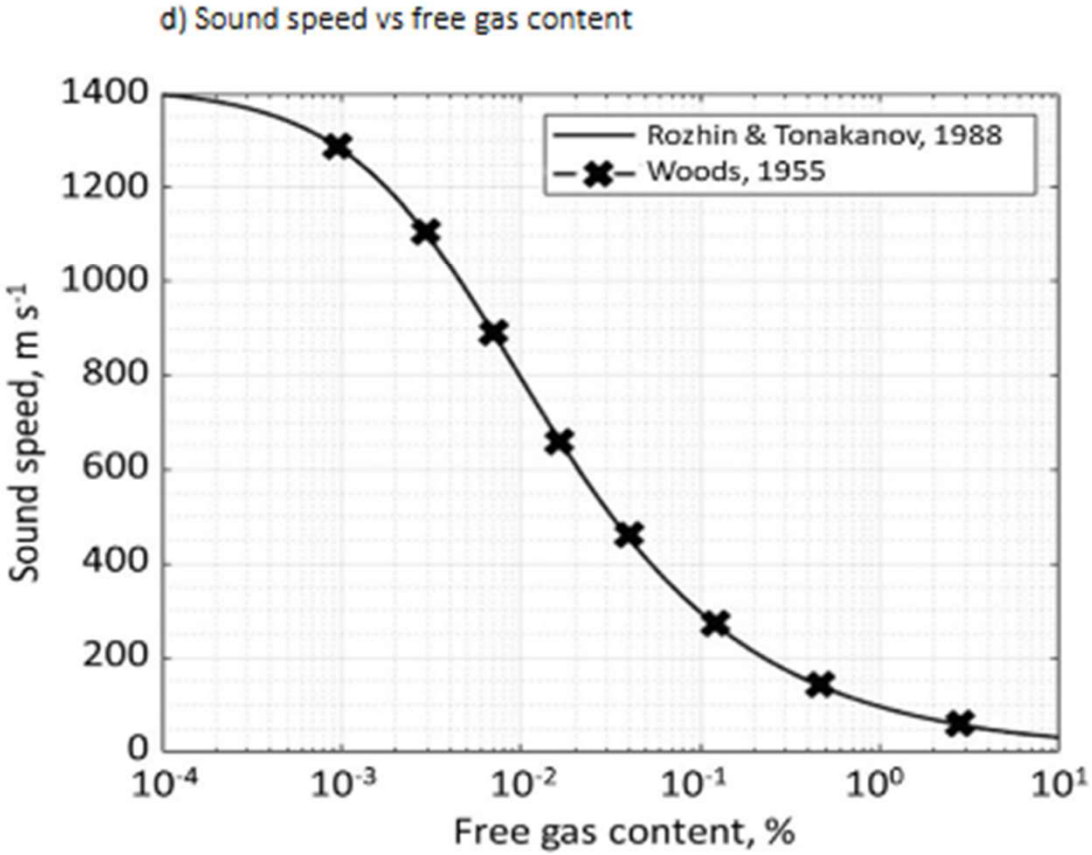
For a reprint

Appendix: following slides NOT shown at SynObs

…. But relate to statements I made

Sound speed, thence lakebed reflectivity, depends strongly on gas fraction

- CH_4 is trapped in the bottom as free gas bubbles and generates a pronounced layer about 0.5 m thick
- 1% of free gas content, Θ, in the sediment
  - decreases sound speed in the sediment by ~15 times (down to 100 m/s) →
  - and increases reflection coefficient by ~5 times
- Uzhansky *et al* **recorded sound reflections from the lakebed to estimate sound speed and free gas content (← "geoacoustic inversion")**



Sound speed, thence lakebed reflectivity, depends strongly on gas fraction

- Uzhansky *et al*
  ernstuzhansky@gmail.com
  ernstu@tauex.tau.ac.il
  recorded sound reflections from the lakebed to estimate sound speed and free gas content (← "geoacoustic inversion")

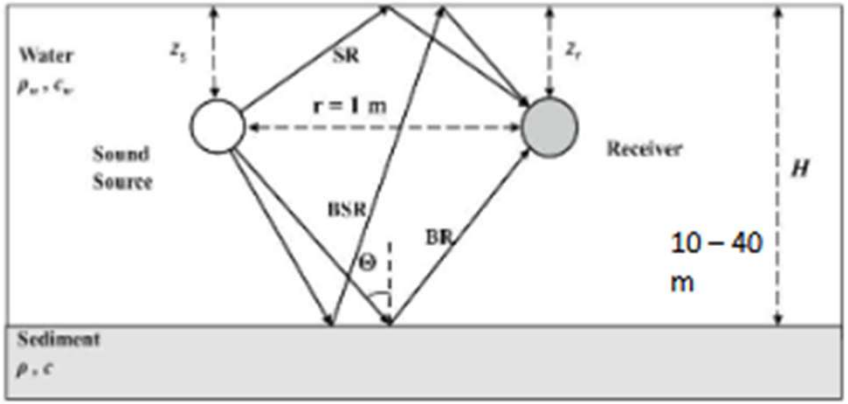
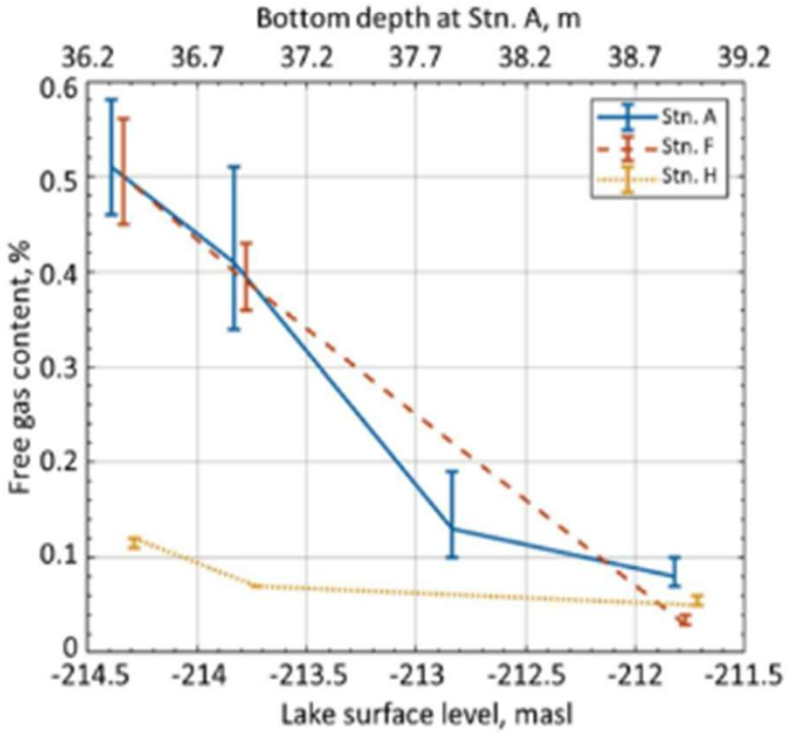


Fig. 5. Geometrical configuration of the experiment.



← Estimated **free gas content as a function of lake level** and corresponding bottom depth at station A

plan "gassy geoacoustic inversion" in L. Biwa !

Research Motivation

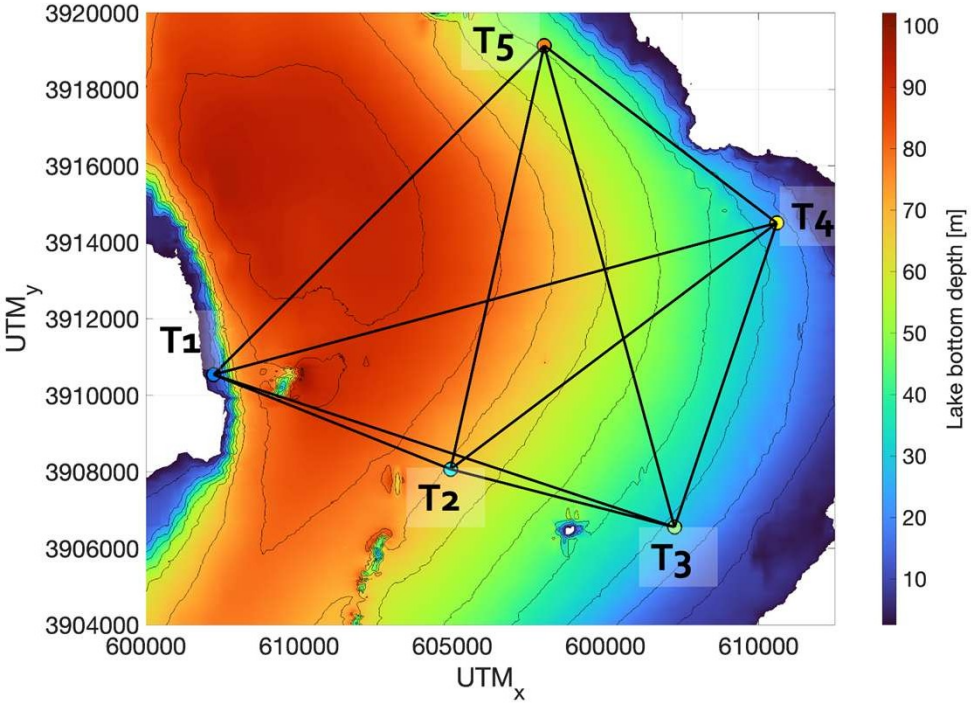
Freshwater resources under increasing stress.
Lakes/reservoirs worldwide are tending to stratify more strongly, often yielding hypoxia , cyanobacterial blooms…

→ v. important to understand these physical changes through field research, and to operationally monitor lakes' physical state (*cf*. Meteolakes forecast L. Geneva).

Overall Target: Nowcast the physical environment in Lake Biwa (water temperature and current fields)

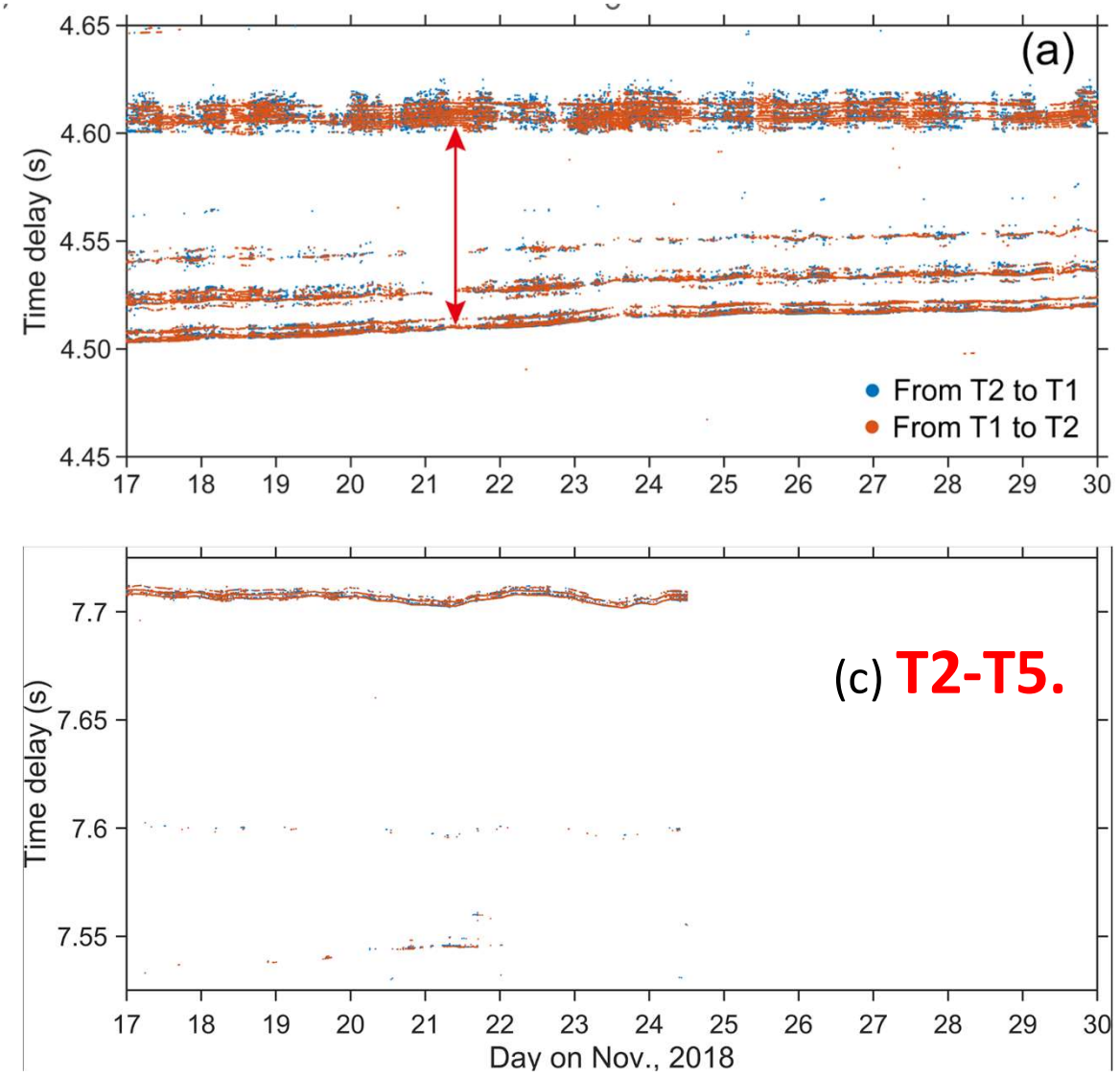
"LB" supplies water to >14 million!

These two arrival groups were found at other transects

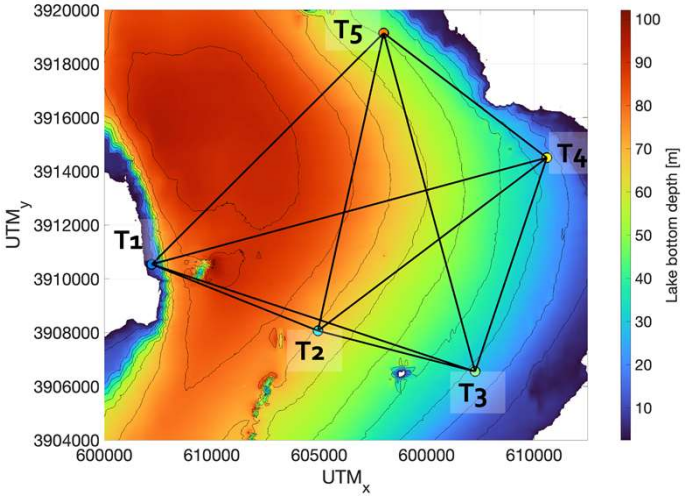


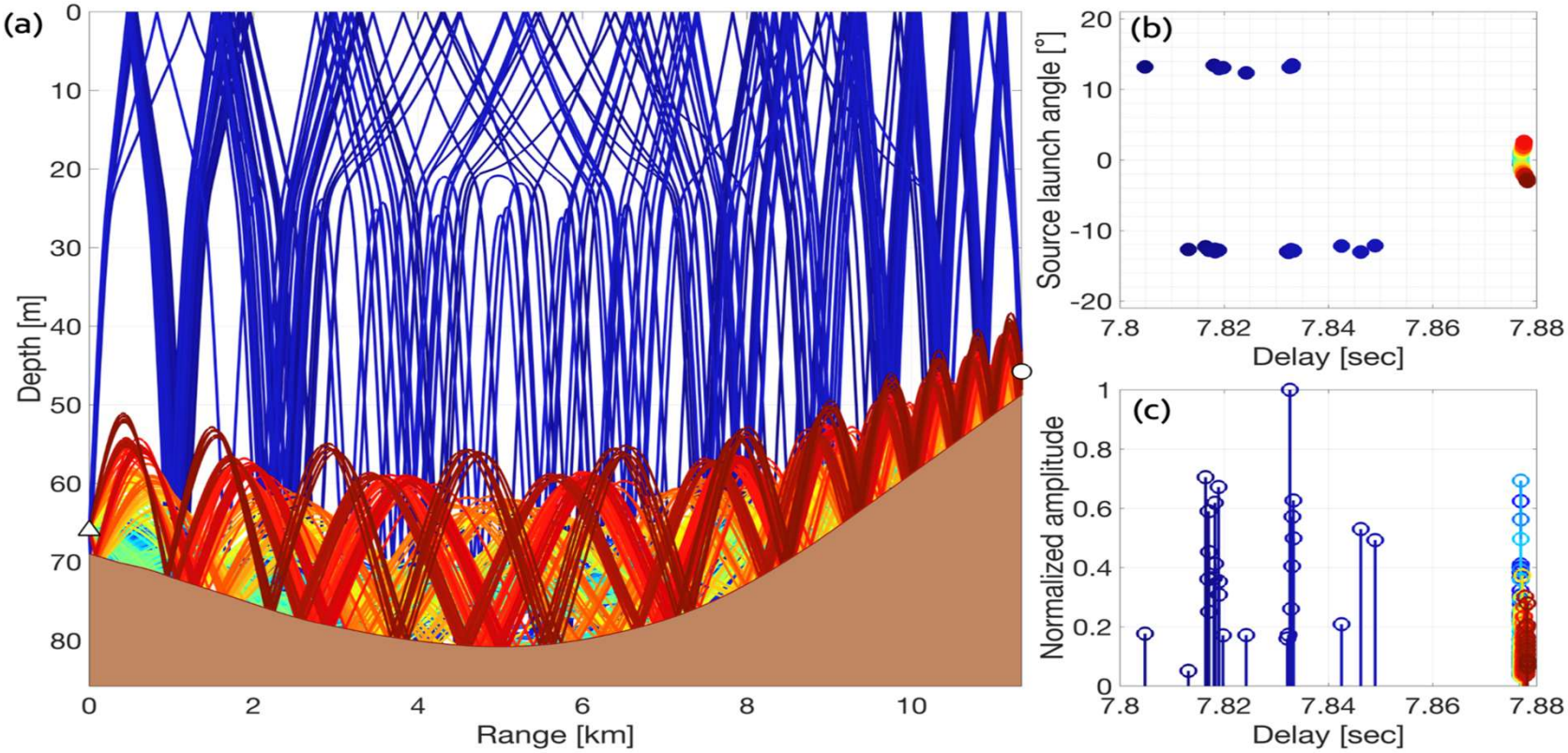
Stn.	T1	T2	T3	T4	T5
T1		6595	12685	15237	12190
T2	17-30*		6097	10560	11147
T3	17-24	16-24		8389	13044
T4	22-30	22-30	22-24		7644
T5	17-24*	22-24*	17-24	21-24	

Reciprocal arrival times versus JST datetime, for (a) **T1-T2**, (b) **T1-T5.** (c) **T2-T5.** **dots where Amp>14dB**



(BELLHOP) Ray tracing results for the T2-T5 transducer pair, based on sound speeds computed from simulated water temperature fields at 00:00 JST, Nov 22, 2018. (a) Ray trajectories for acoustic path from T2 to T5. Simulated arrival times versus (b) source launch angle and (c) normalized ray amplitude. Eigenrays are color-coded by arrival time. Positive launch angles downwards





→ Qualitatively at least, supports existence of *weak* surface channel and deep channel

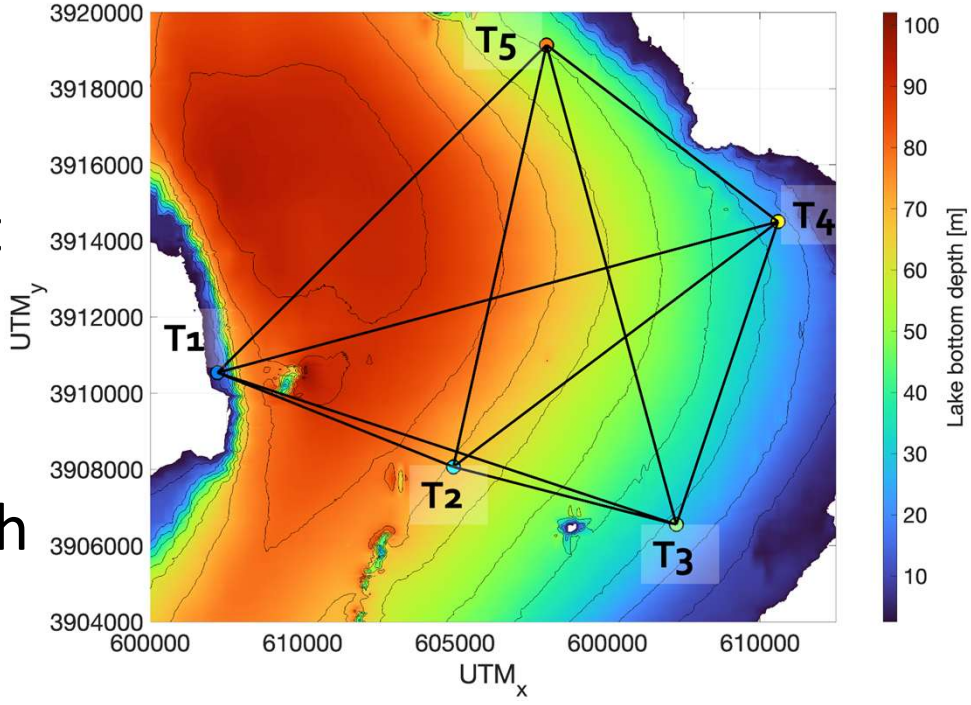
When do both surface and deep channels appear?

Only transects T1-T2 , T1-T5 and T2-T5 yielded arrivals of both types, *i.e.* with “progressively slowing” and “quasi-constant” arrival time.

What made these three transects special?

T2 and T5 both lay below the thermocline (@z=35 m), the only such combination → It is natural that they could communicate through the hypolimnion, whose near-constant temperature yielded “quasi-constant” arrival time.

As for T1-T2 and T1-T5, only one of their transducers lay below the thermocline. We tentatively propose that the steep slope just offshore of T1 formed a privileged conduit for sound, by which the transducer at T1 communicated strongly with both the epilimion and hypolimnion, and thereby with the deep transducers T2 and T5 by both shallow and deep routes.



Nov. 2017; stratified conditions

E station to Takeshima (“land-based” deployment);

TR 2.5 m above Bottom@49 m. (~7 sec ping).

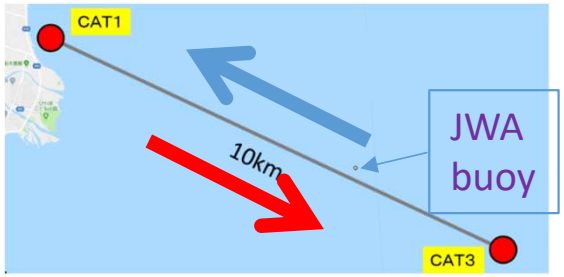


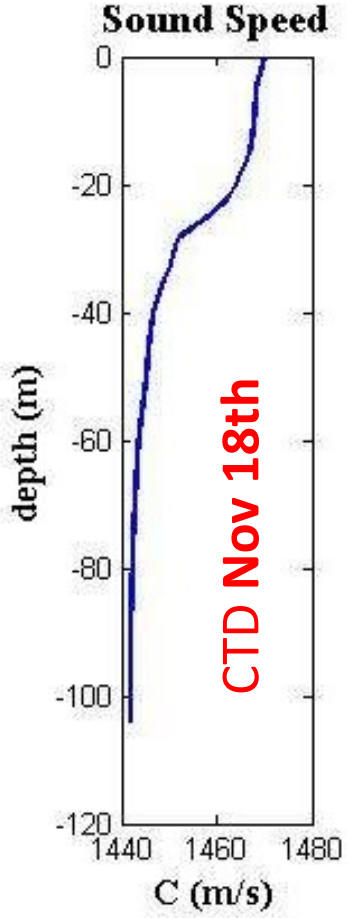


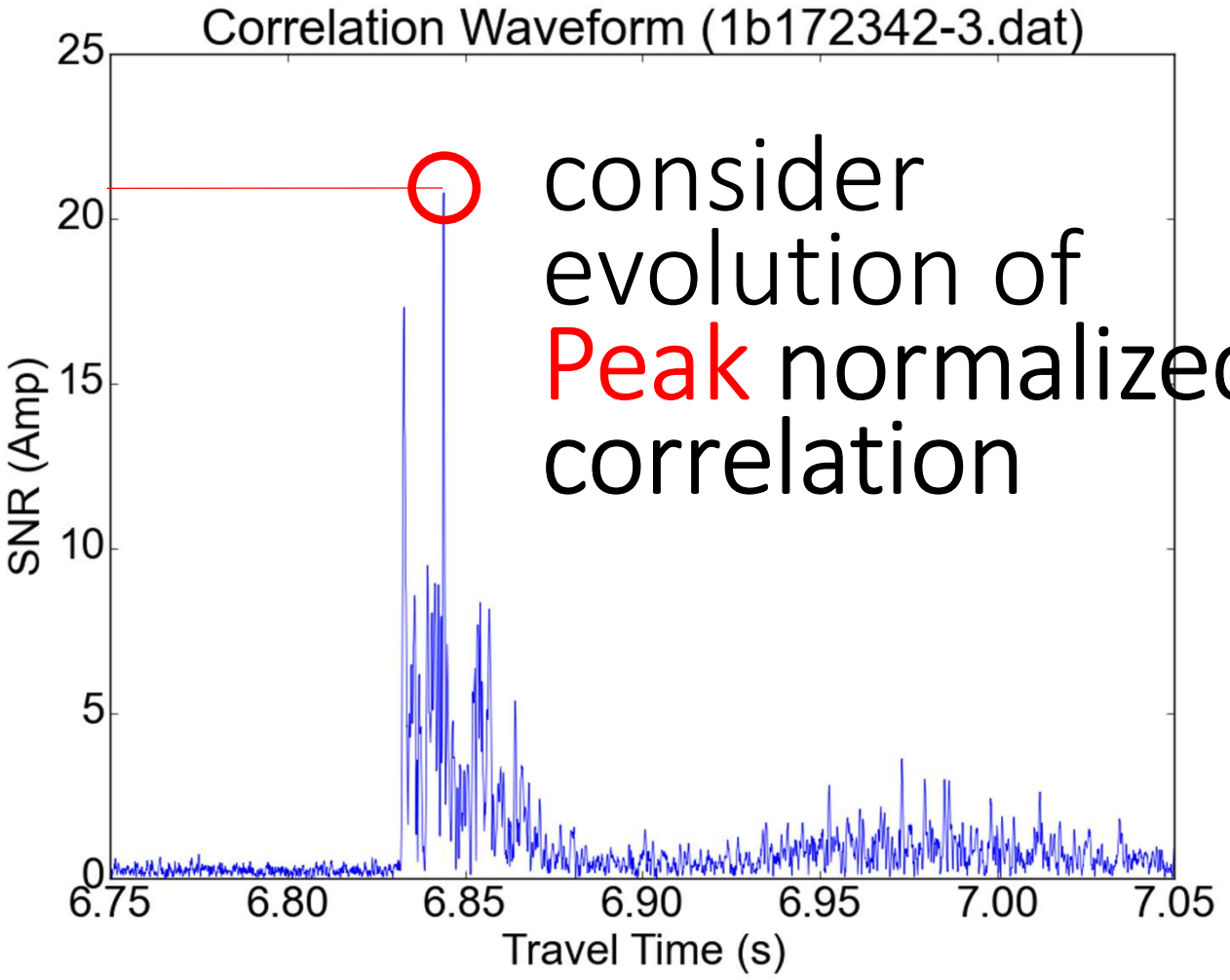
Show cross-sec

bathymetry!!!

Nov ’17 “stratified” trials





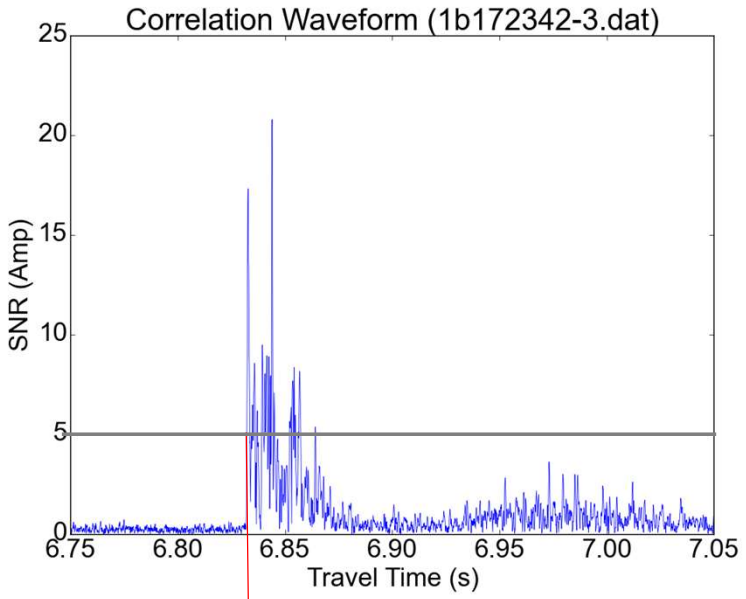


consider evolution of Peak normalized correlation

Note multiple peaks in correlogram!

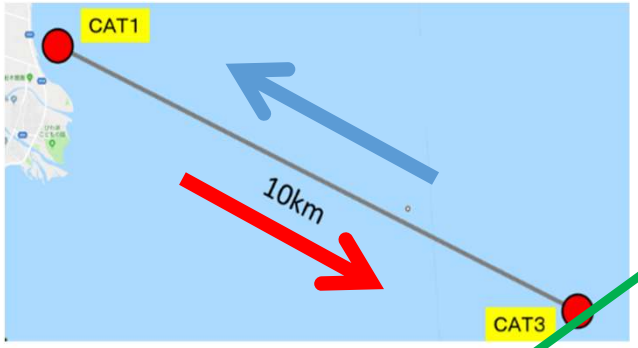
→ so we'll judge acoustic "arrival time" by a threshold exceedance time

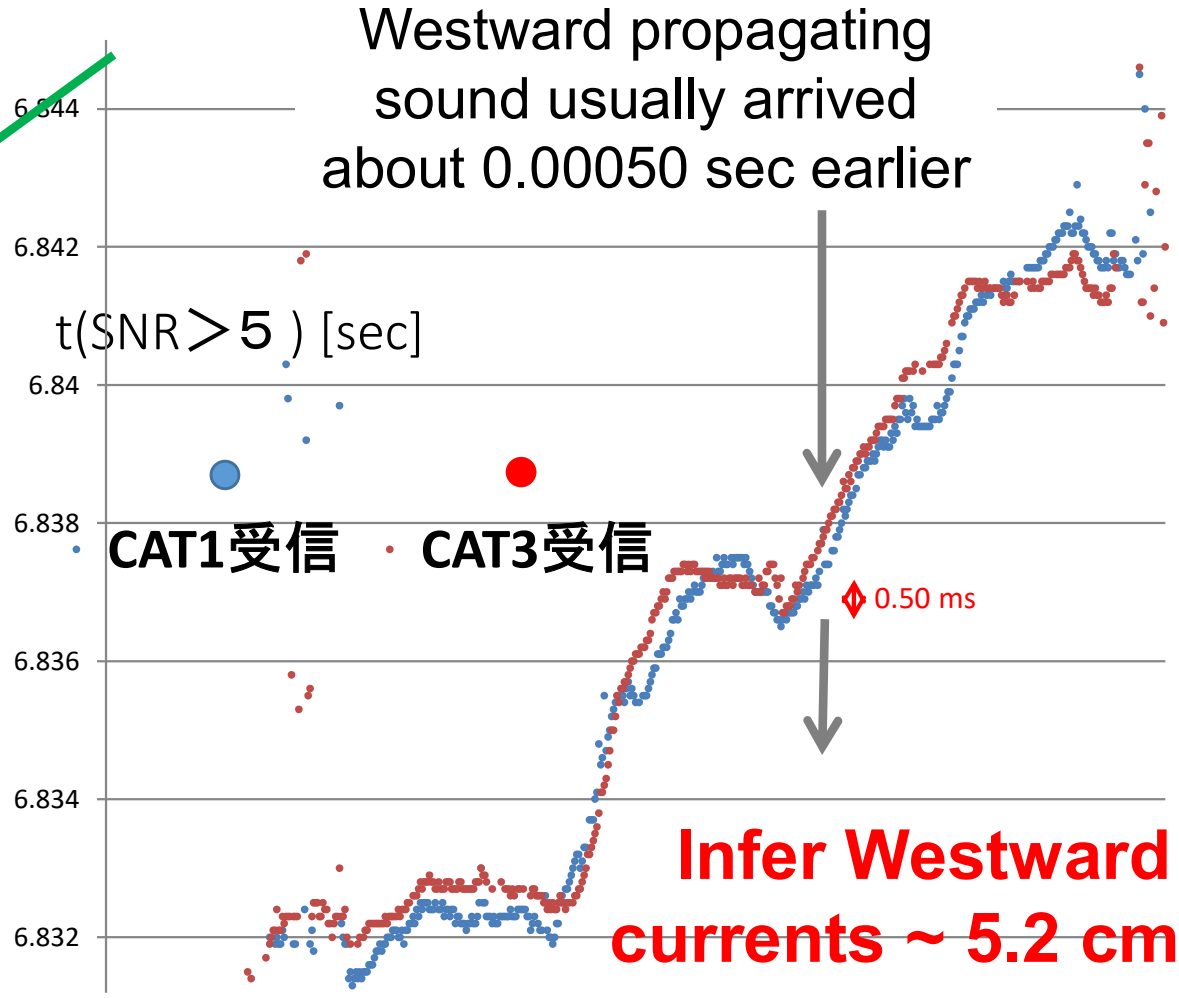
Next slide shows how this time evolved



$t_{SNR>5}$

Differential Travel Time (DTT)





2017/3 Attempts to improve confidence in estimates of DTT suggest **that "bulk phase differences"** (Spiesberger *et al* 1989) provide robust, complementary information that is less sensitive to fade-ins/outs by interference of micromultipaths → *continuing work*